The Abdus Salam
International Centre for Theoretical Physics

United Nations
Educational, Scientific and
Cultural Organization

IAEA
International Atomic Energy Agency

2245-14

Joint ICTP-IAEA Advanced School on the Role of Nuclear Technology in Hydrogen-Based Energy Systems

13 - 18 June 2011

Hydrogen in metals: impacts on thestructural, mechanical & magnetic properties

Daniel Fruchart
Institut Neel, CNRS
Grenoble
France

Hydrogen in metals : impacts on the structural, mechanical & magnetic properties

Daniel FRUCHART
Institut Néel, CNRS, Grenoble, France

Joint ICTP-IAEA Advanced School on the Role of Nuclear Technology in Hydrogen Based Energy Systems

Main interests

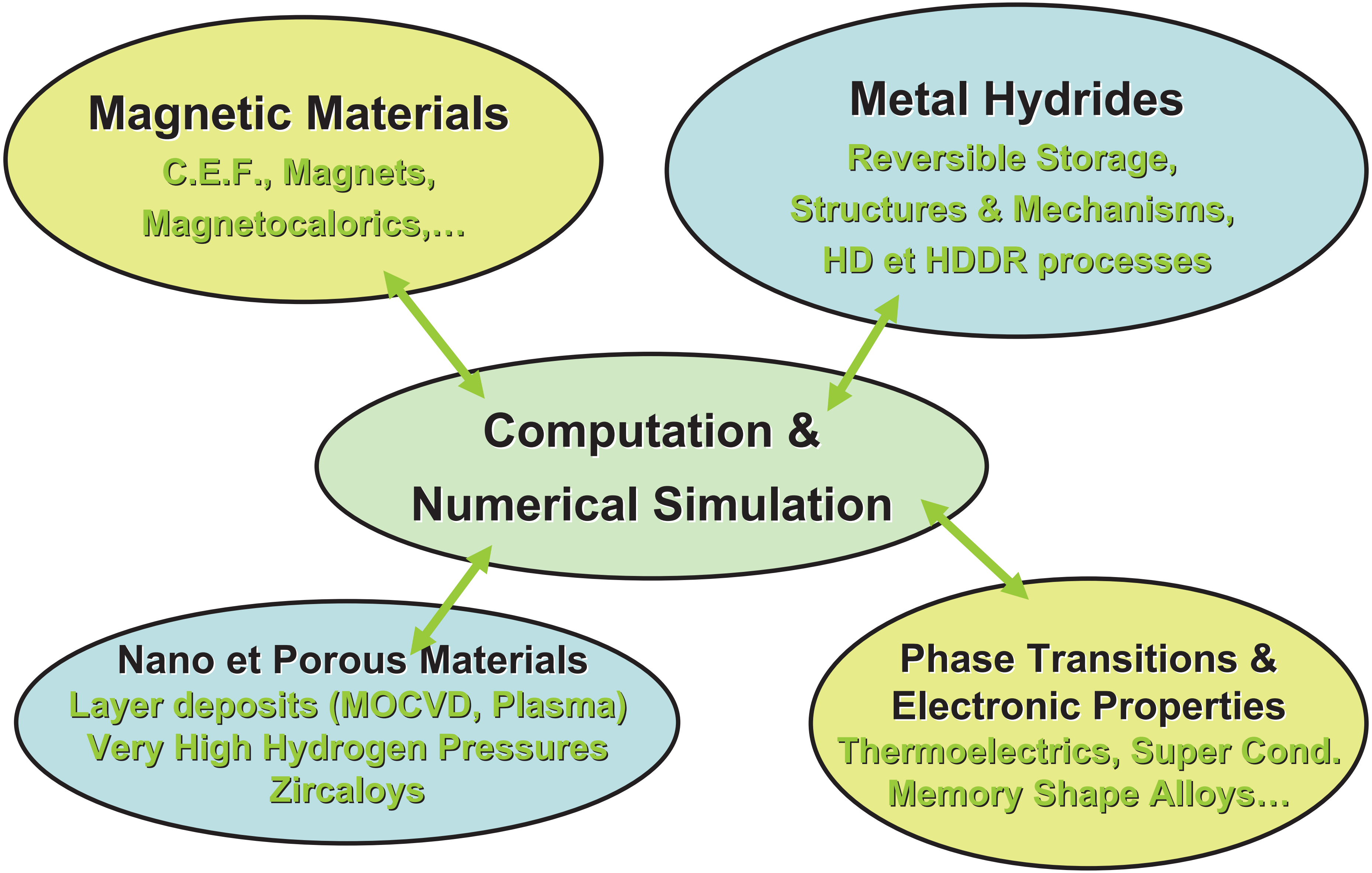

Hydrogen reversible storage as metal hydrides

→ Hydrogen

- **Storage of electrical and chemical energies** (electrolysis, thermochemistry)
- **FC** (high efficiency, no polluant)
- **ICE** (pollution réduite)
- **High mass energetic density**

Production-distribution-storage-use

→ **Reversible Metal Hydrides**

Safe storage, high vol. density, pure H_2 (FC)

	kg H_2 / m^3	% massique
H_2 gaz 700b	62	100
H_2 Liq.	70	100
$LaNi_5H_6$	123	1.4
Ti-V-Cr	205	3.5
$AlNaH_4$	96	7.5
MgH_2	106	7.6

Metal hydrides - BCC type alloys

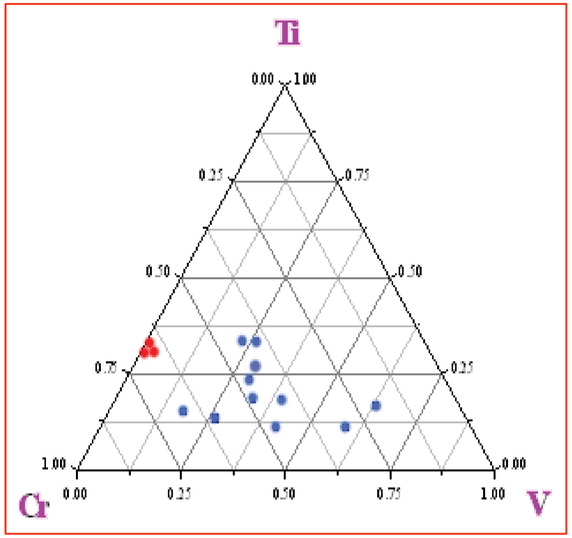

$TiV_{0.8}Cr_{1.2}$ x_{max} ~ 3.1w%.... up to…

$Ti_{0.5}V_{1.9}Cr_{0.6}$ x_{max} ~ 3.6w%

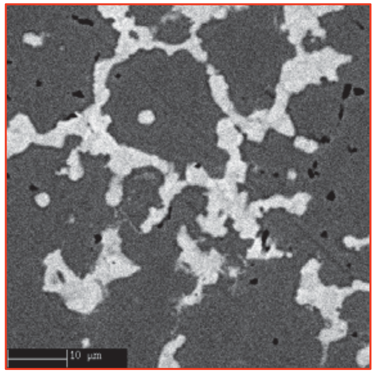

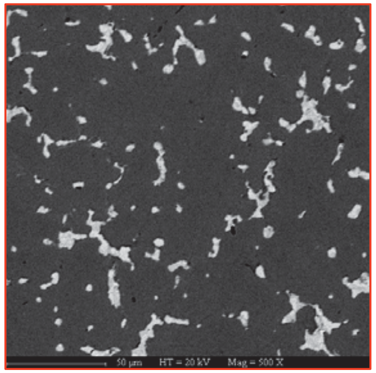

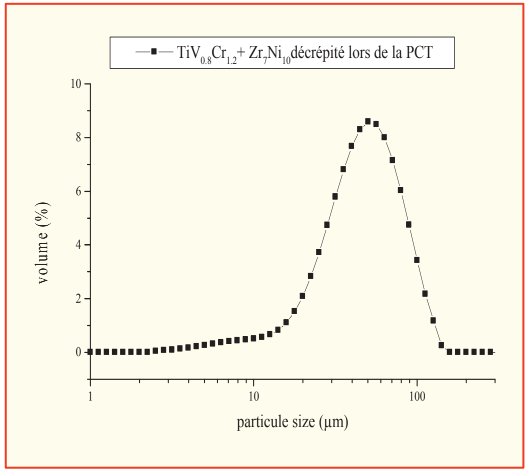

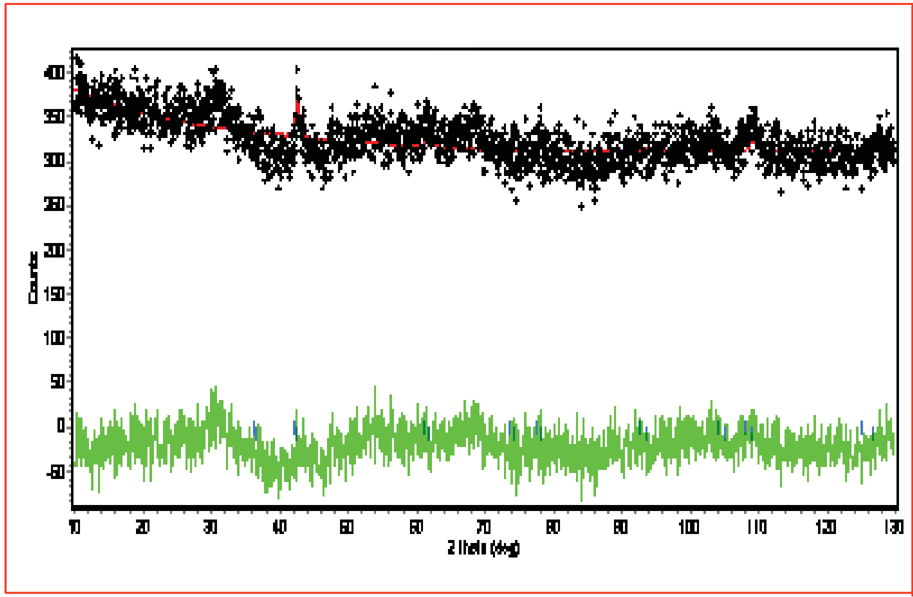

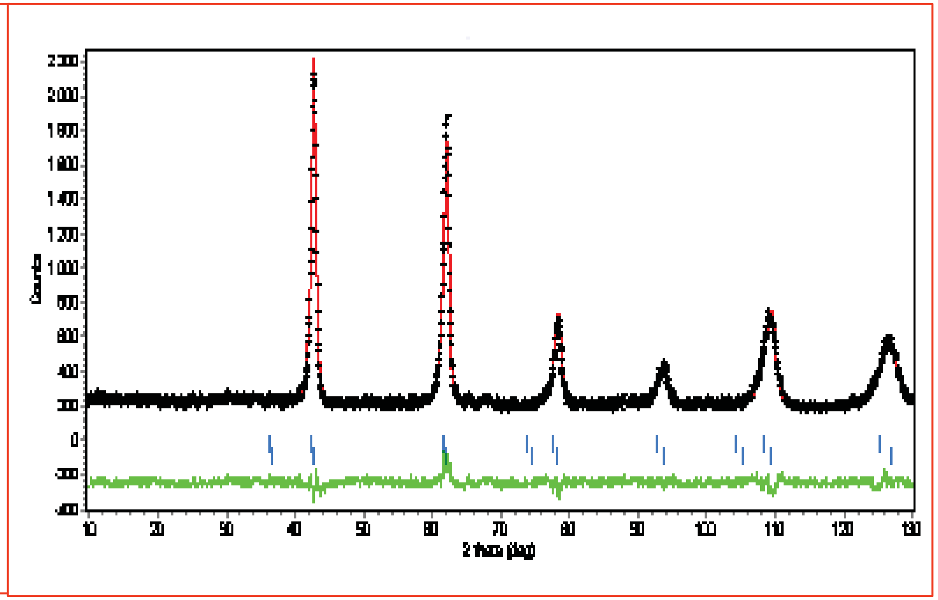

Mg vs MgH_2

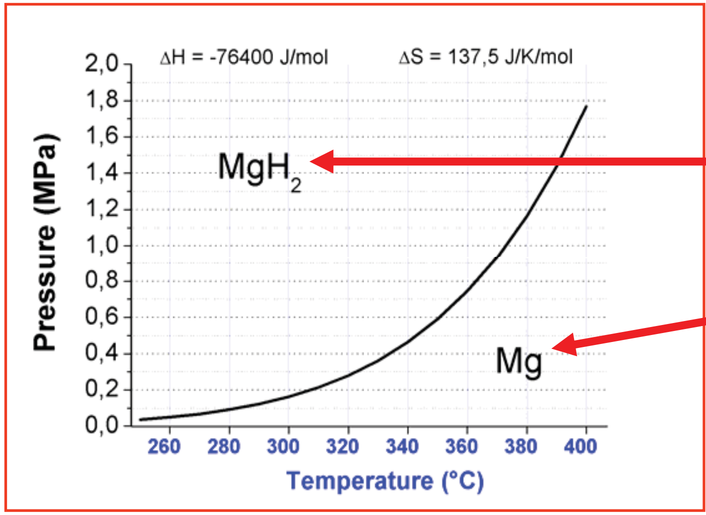

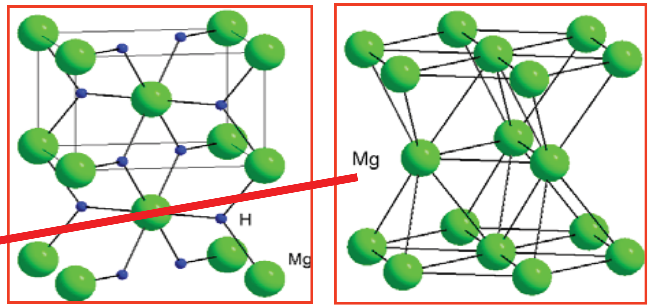

β-MgH_2 rutile type   Mg metal - hcp

<u>So called difficulties with Mg</u>

H-reaction kinetic are said low, but…

Temperature of reaction is high, but…

<u>Mg is the best ?</u>

Mg is the 7th most abundant element on earth

Mg has ~ same cost as Al

Mg metallurgy is easy

Mg is bio-compatible

Mg is re-cyclable

MgH_2 is monometal hydride system: no demixtion

MgH_2 uptake is 7.6 w%

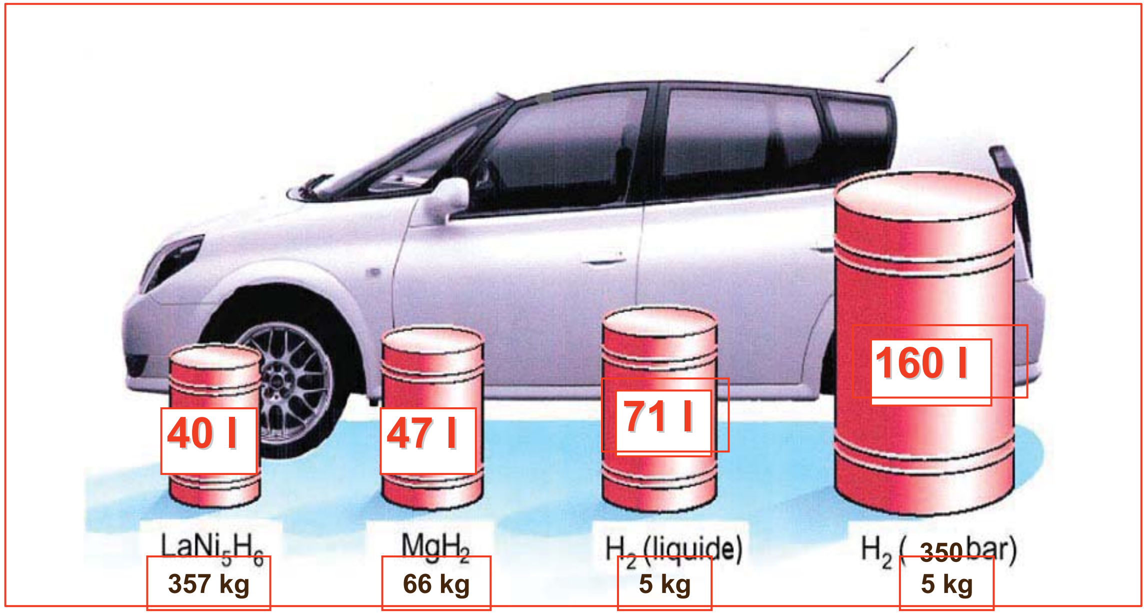

Tank : 5 kg H_2 = 300 km

Connection of a 2 kg MgH_2 tank to applications

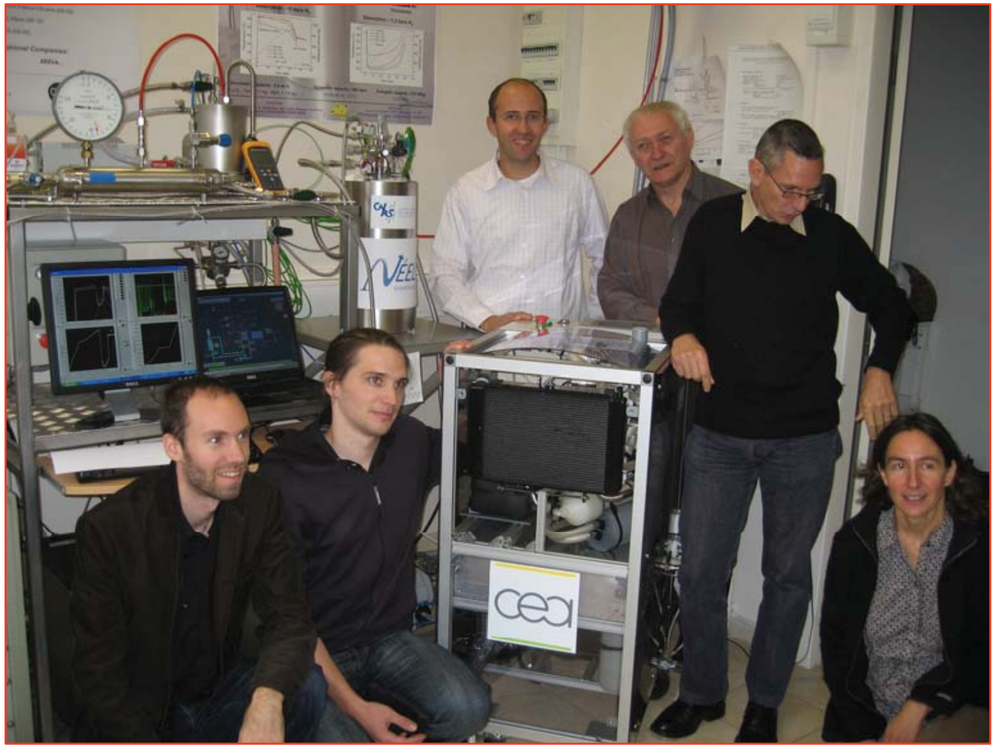

Connection to the «EPICEA» PEM-FC of CEA, Grenoble (4 kW, effic. ~ 50%, 2 kW electric) here powering for ~ 1 h. a ancillary heater

Direct H_2 gas fuelling a lawn-mower from the MgH_2 tank powering as well the PEM-FC

Autonomous tank under development

Porous Membranes
bi - catalytists

Nanostructures built under high hydrogen pressure (5 GPa) via demixtion of a Pd (Pt, Rh) + 2% Ce (Zr, Al) alloy

Creation of oxydes nanocrystals (catalytist)
In a platinoïd matrix (catalyst)

CeO_{2-x} epitaxied on Pd

Matrix Pd

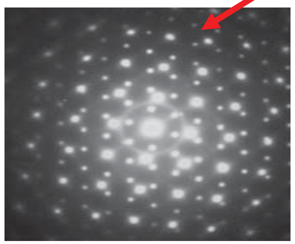

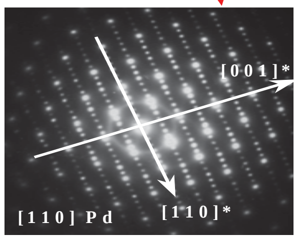

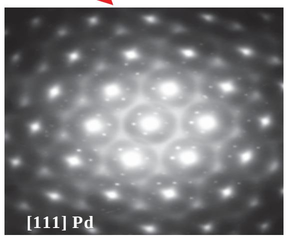

Antiphase structure
Ce-O & PdO

Diluted Ce (2%) clusters

EXAFS

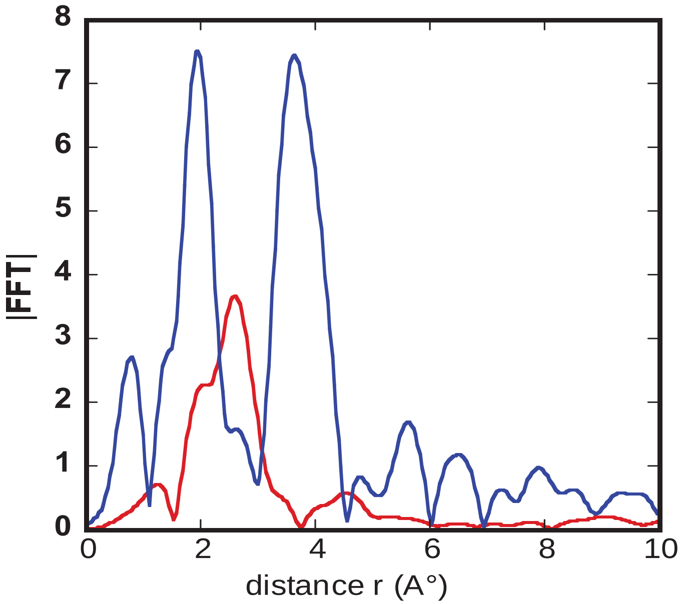

Before oxidation : SS
After oxidation : CeO_{2-x}

Also

Hard Magnetics (fundamental and applications)

Magnetocaloric materials

Magnetostrictives

Soft magnetics

Shape memory materials

Thermoelectrics

Thin layers

Zircaloys

European Collaborations

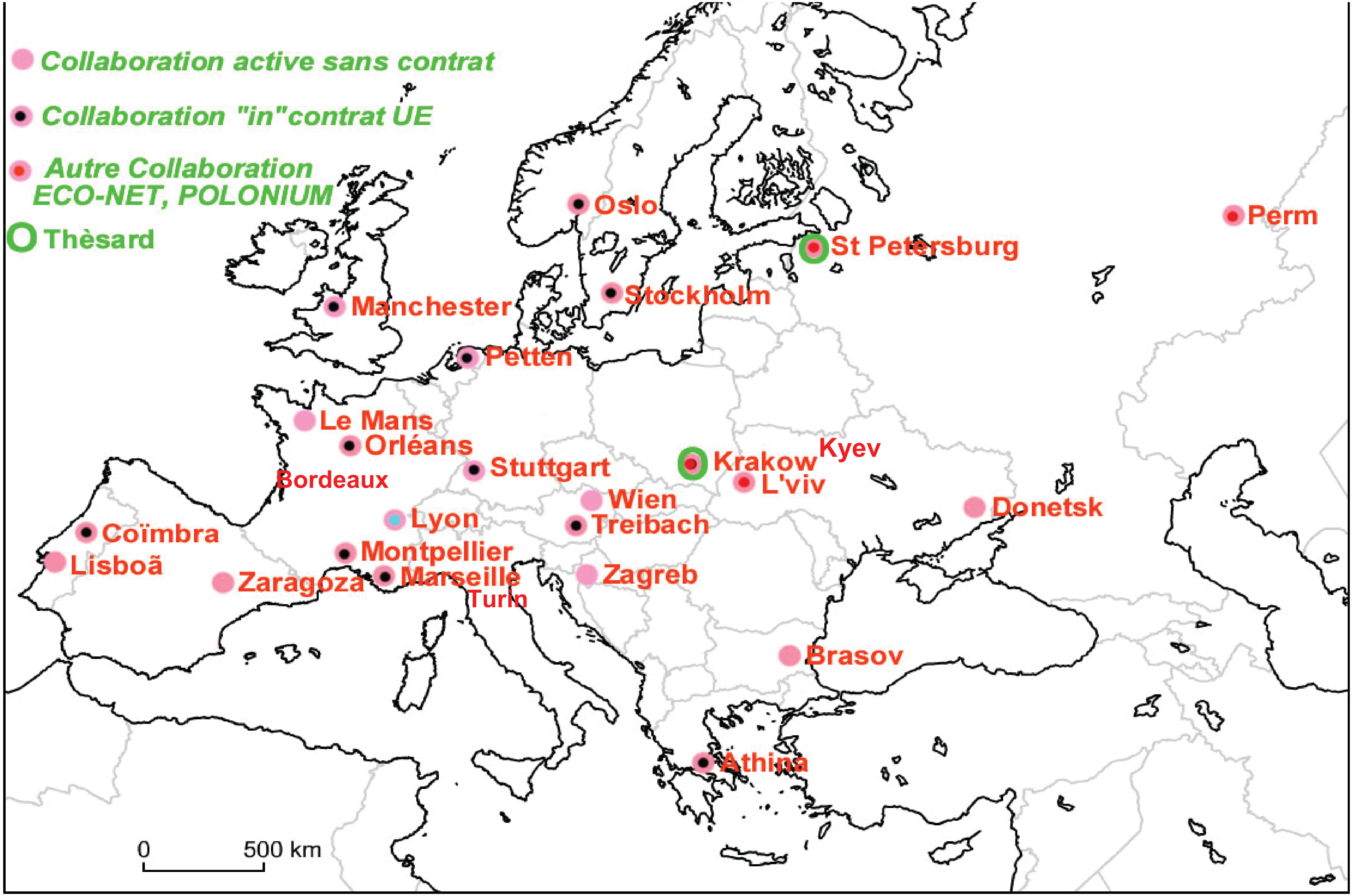

International Collaborations

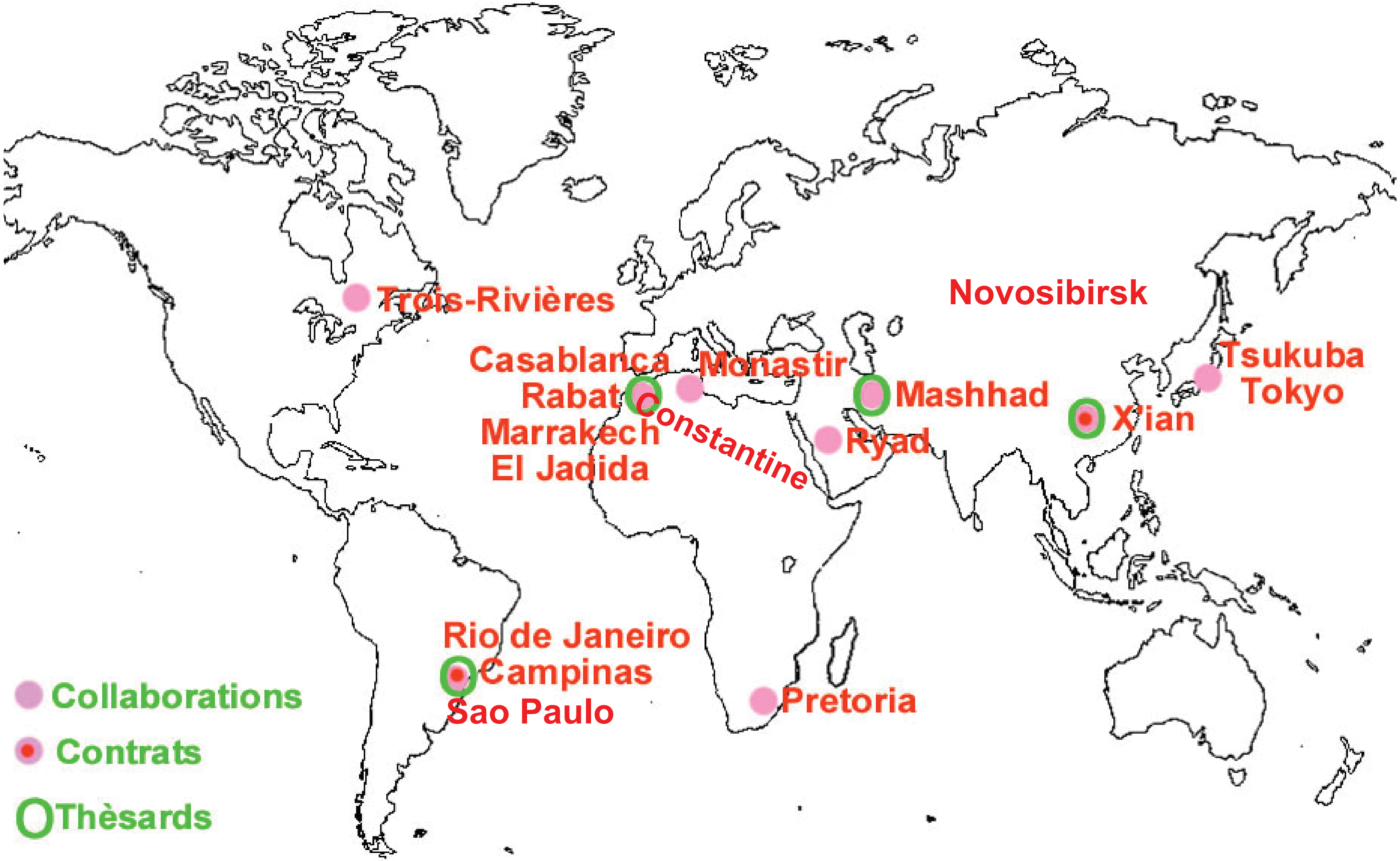

Hydrogen in metals, impacts on the structural, mechanical & magnetic properties

Main principles

- Structure and mechanical aspects
- Electronic (Magnetic) aspects

Experimental analysis

- Neutron scattering (and X-rays)
- Spectroscopy techniques

Theoretical approaches

Intrinsic effects at microstructure and structural scale

Impacts on fundamental properties

Extrinsic properties

METALIC HYDRIDES

HYDROGEN INTERCALATION IN METALHYDRIDES

HYDROGEN
ON
TETRAHEDRAL SITES

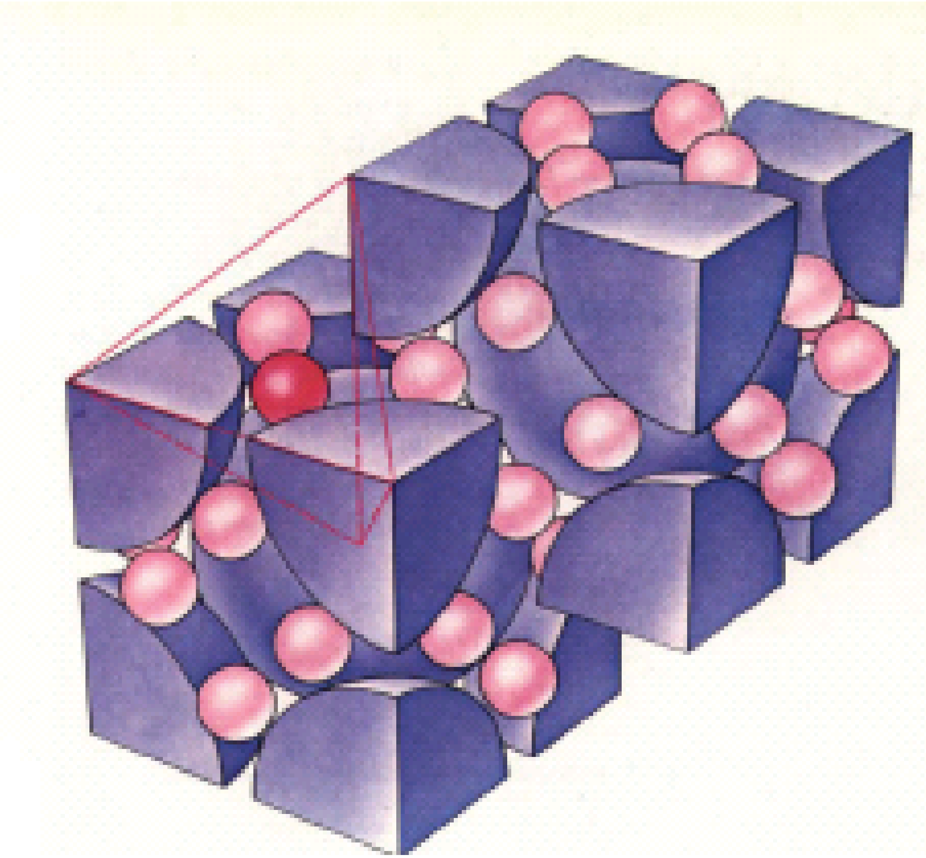

HYDROGEN
ON
OCTAHEDRAL SITES

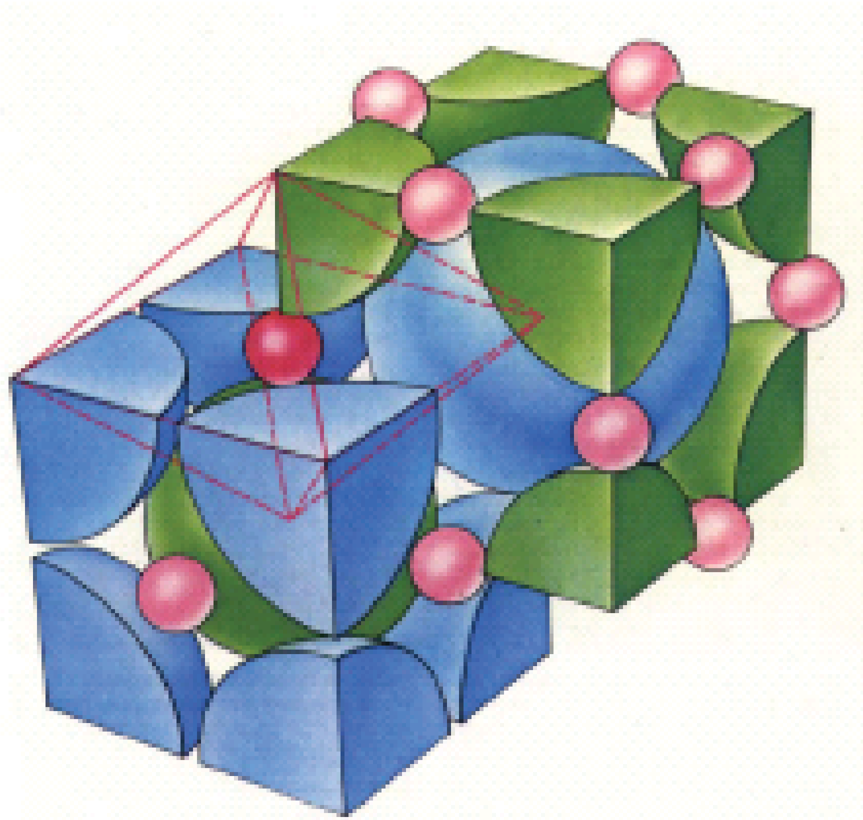

HYDROGEN ABSORPTION

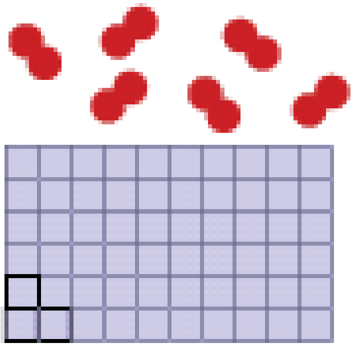

Hydrogen gas

Metal

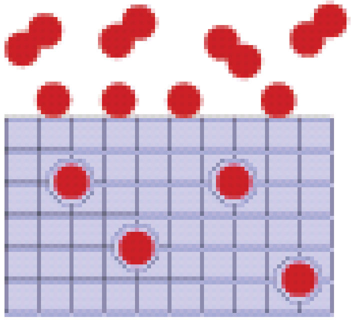

α-Phase: Solid Solution

$MH_x \quad (0 < x < 0.1)$

$\cancel{H \leftrightarrow H}$, $\Delta V/V = k \cdot c_H$

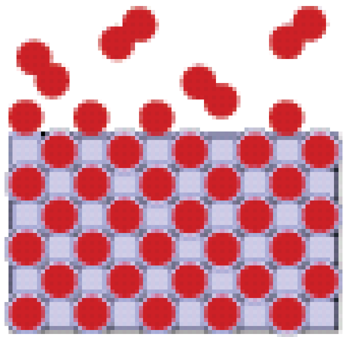

β-Phase: Hydride Phase

$MH_x \quad x = \{1, 2, 3, \ldots\}$

$H \leftrightarrow H$

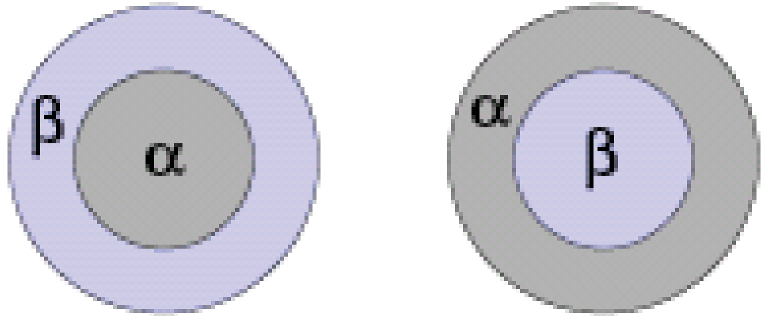

Absorption

Desorption

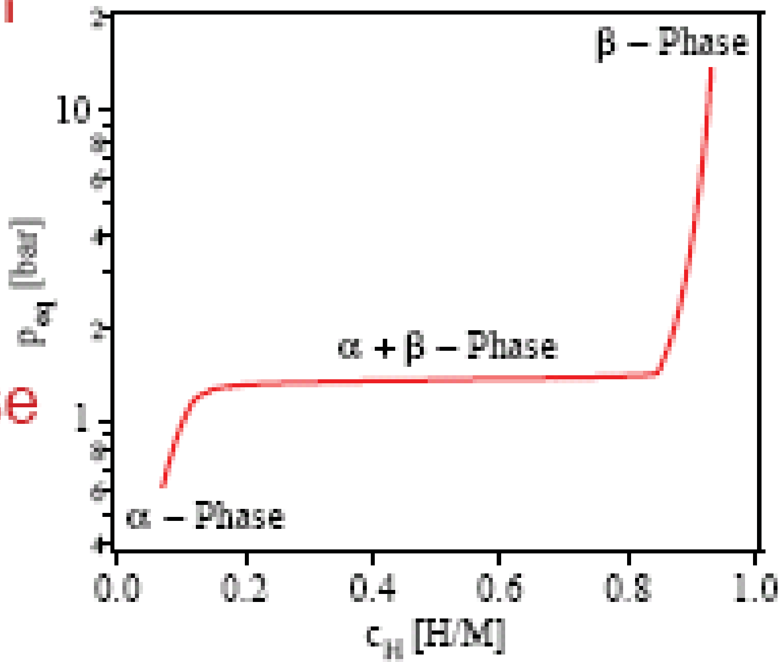

BINARY HYDRIDES

MAGNETIC ELEMENTS

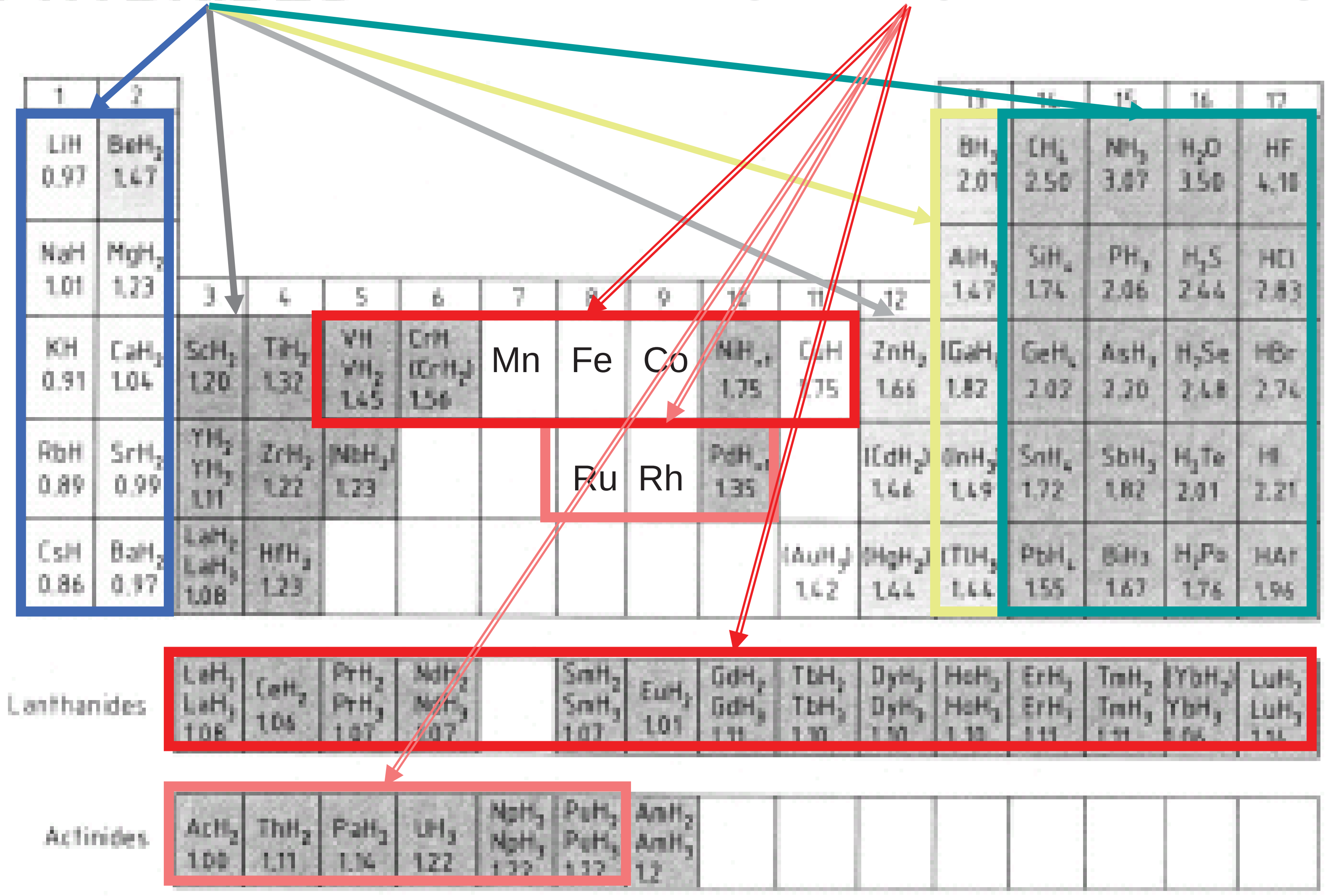

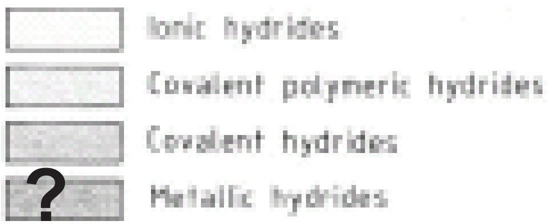

Figure 1. Periodic system of binary hydrides (the figures in the table are the Allred–Rochow electronegativities) Hydrides in parentheses are unstable at ambient temperature.

MULTINARY METAL HYDRIDES ?

PHASE TRANSITION

$$R \cdot T \cdot \ln\left(\frac{p}{p_0}\right) = \Delta H - T \cdot \Delta S$$

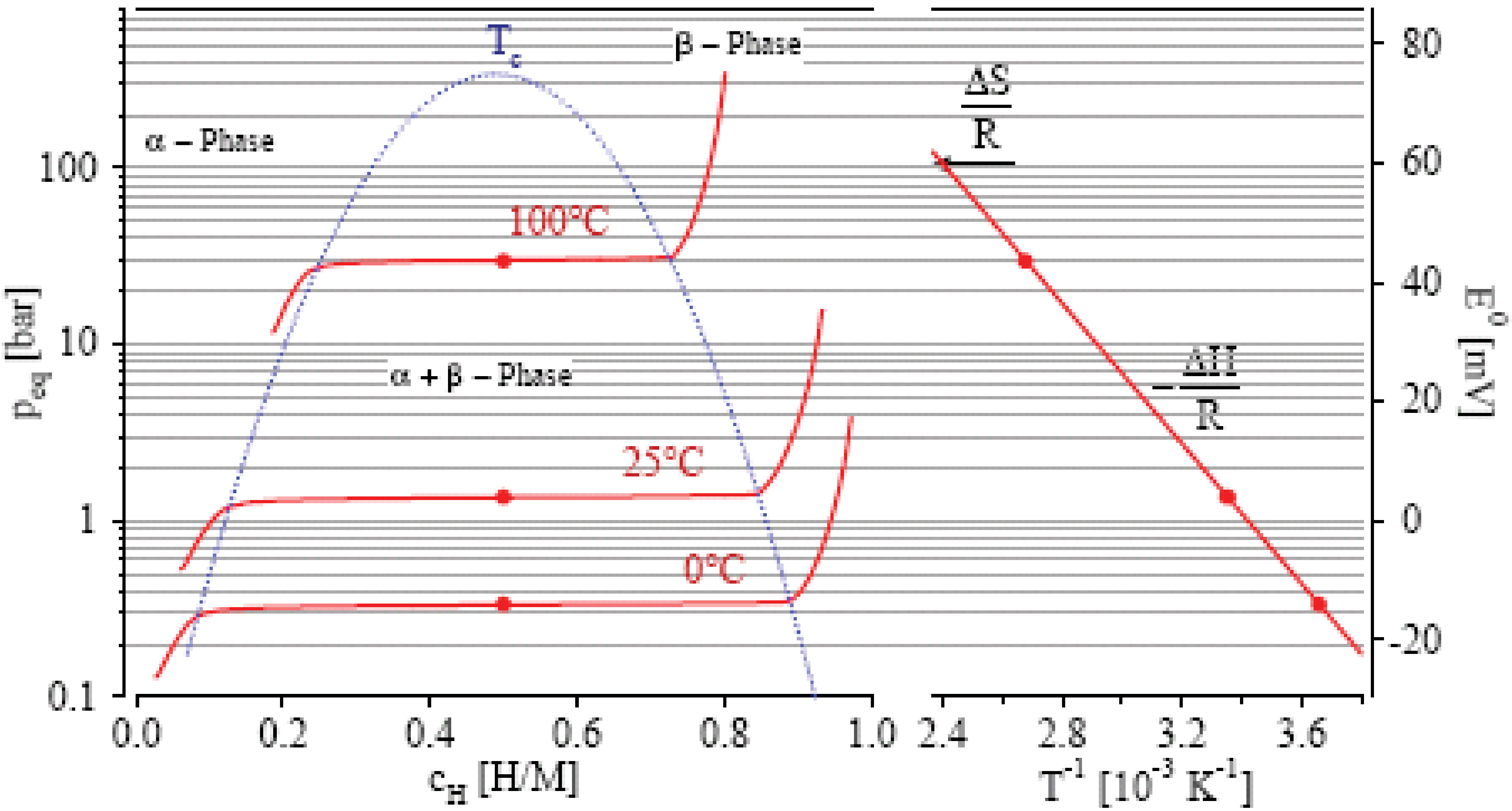

VAN'T HOFF PLOT OF METAL HYDRIDES

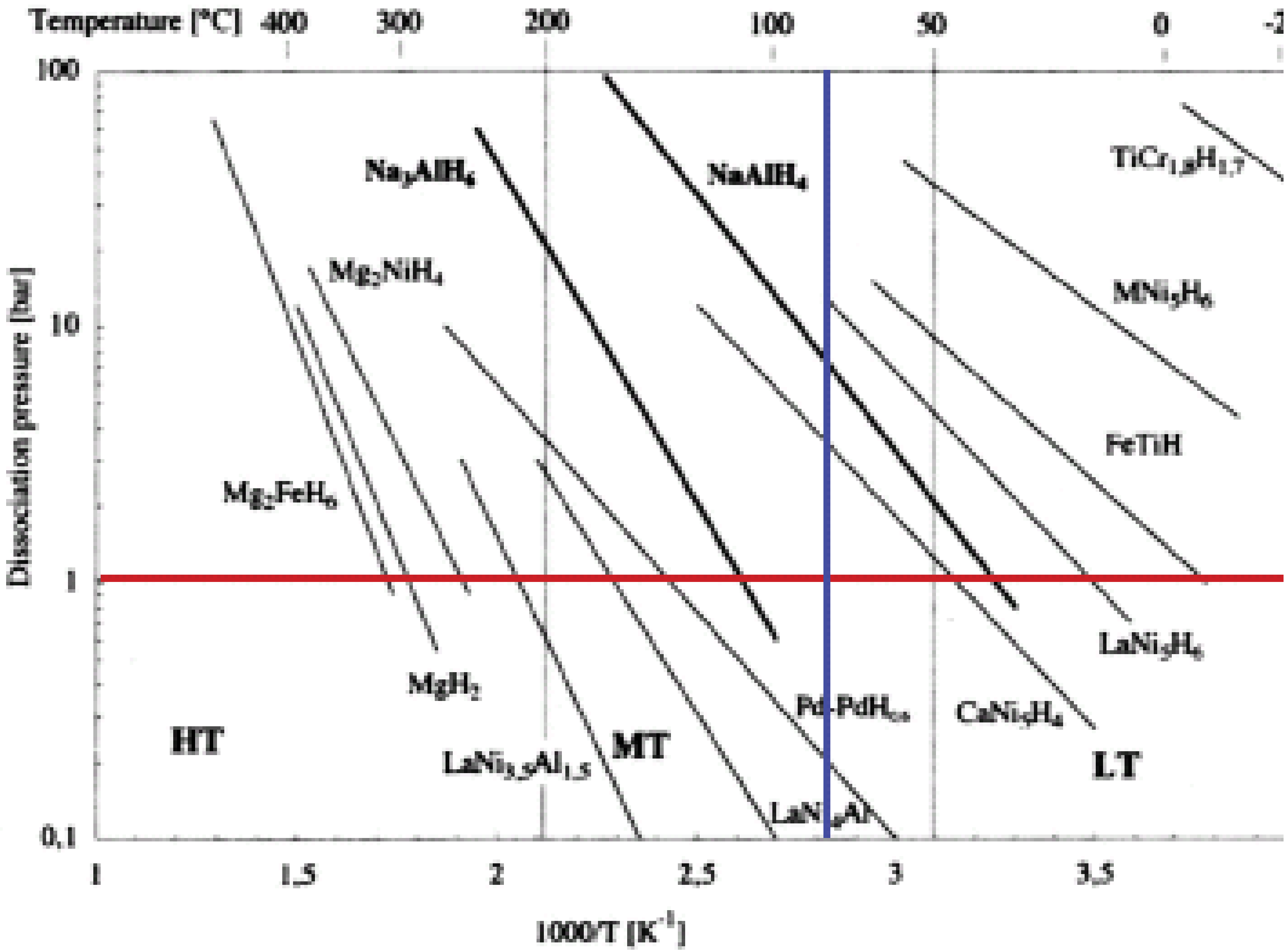

Figures of merit

r(mol.) > 1.4 Å

r(H^-) = 2.1 Å

r(H^0) = 0.529 Å (Bohr)

r(H^+) = 0.16–0.38 Å

r($_{insert}$) > 0.4 Å (Westlake)

d(H-H) > 2.1 Å (Switendick)

V(H) ~ 2.7–2.9 $Å^3$

ΔV/V: from few % up to 30 %

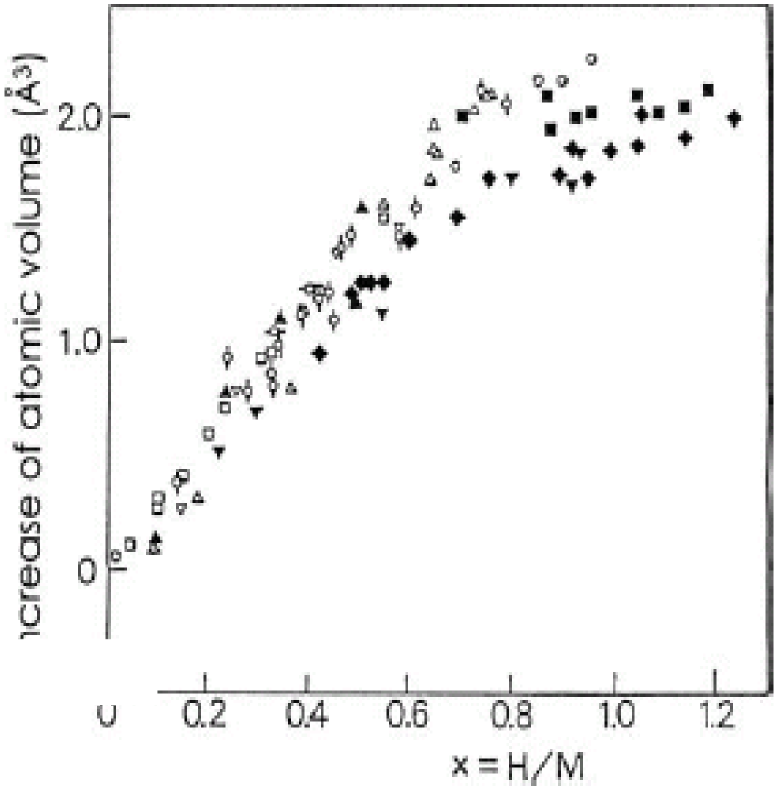

] Volume increase due to H in fcc metals and alloys. ○: Pd, ×: Pd–Cu, +: Pd–Ag, □: Pd–Au, ∇: Pd–Ir, △: Pd–Pt, ▲: Cu–Ni [4.29]; ■: Ni, ♦: Ni–Fe, ▼: Fe–Ni–Mn [4.64]

compare to relative volume expansion at a magnetic transition ! ;

a few ‰ to ~1%

Structural to mechanical microstructure transformations

Coherent vs incoherent volume expansion

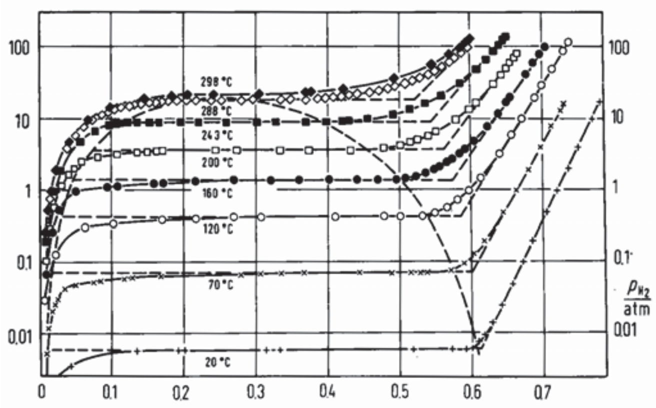

$p(n)$ isotherms of Pd(H) with bulk palladium at different temperatures

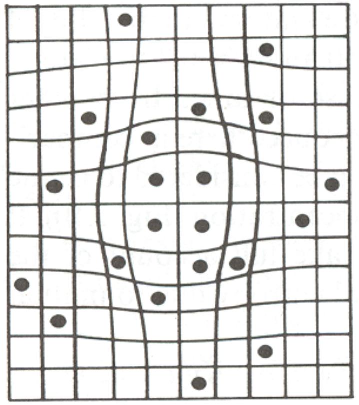

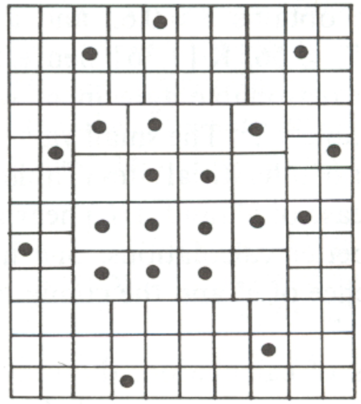

Displacive vs distortive transformations

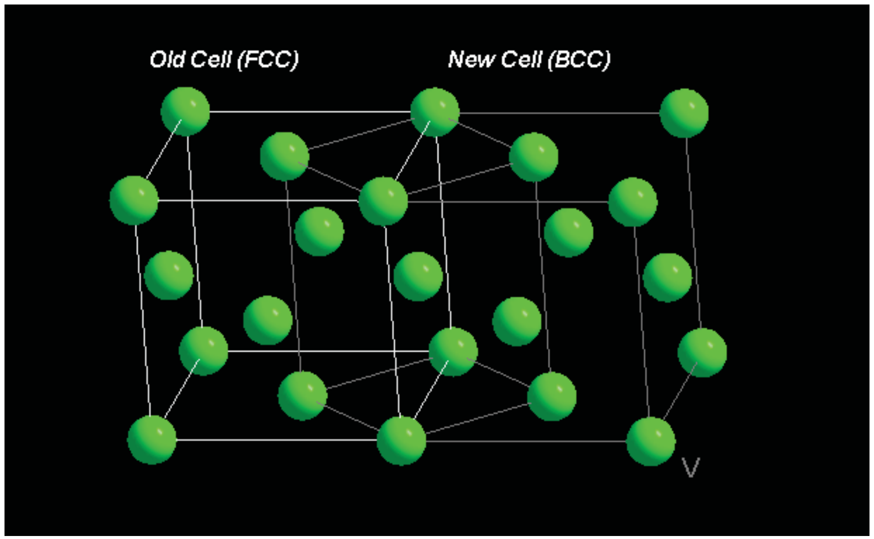

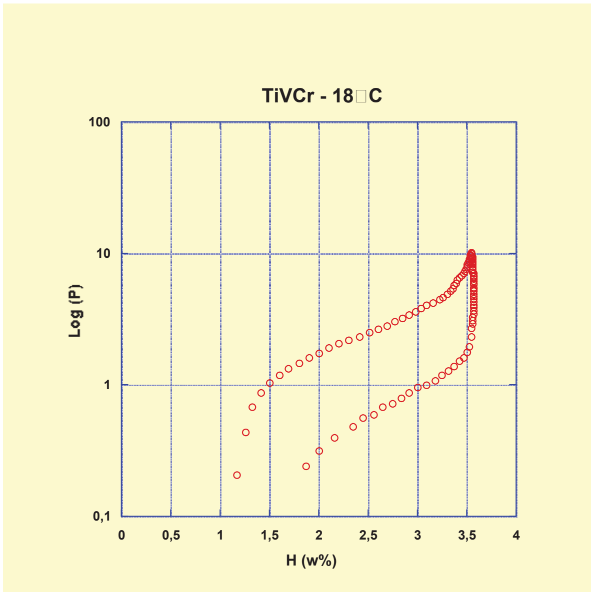

Structure changes

1- RE (hcp) ↔ REH_2 (fcc) ↔ REH_3 (hcp)

2- $TiCr_2$ – C15 (fcc) ↔ $TiCr_2H_5$ – C14 (hcp)

3- β-$NbH_{0,89}$ → α'-$NbH_{<0,89}$ → α-$NbH_{\sim 0,2}$

Orthorhombic Superstructure **Non mobile H**

Disordered Phase **Mobile H** (vacancies)

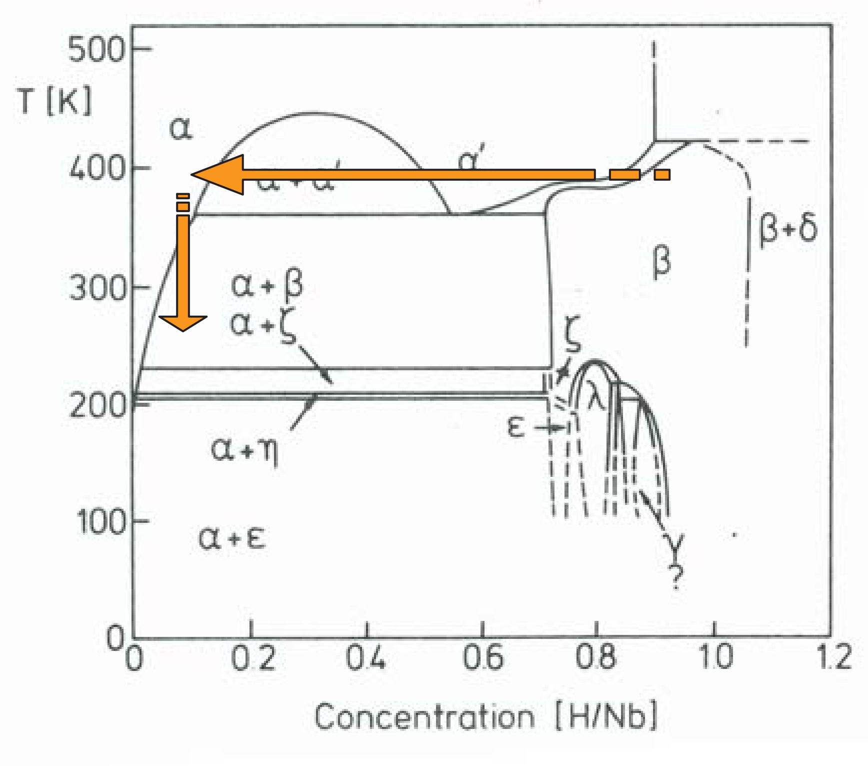

Microstructural effects

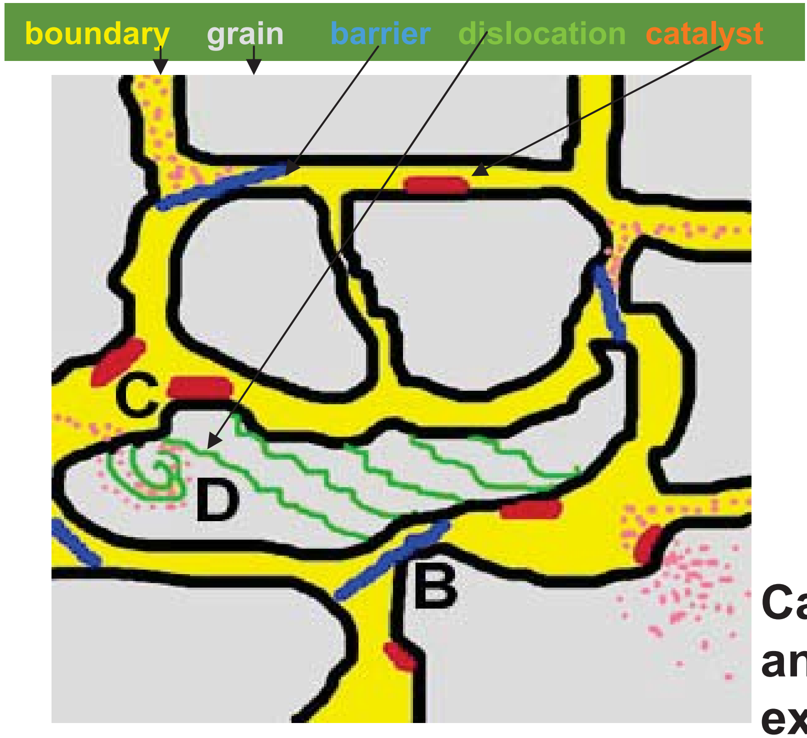

Can affect all components of a composite alloy and more particularly its physical intrinsic and extrinsic characteristics

BCC type alloys (compound)

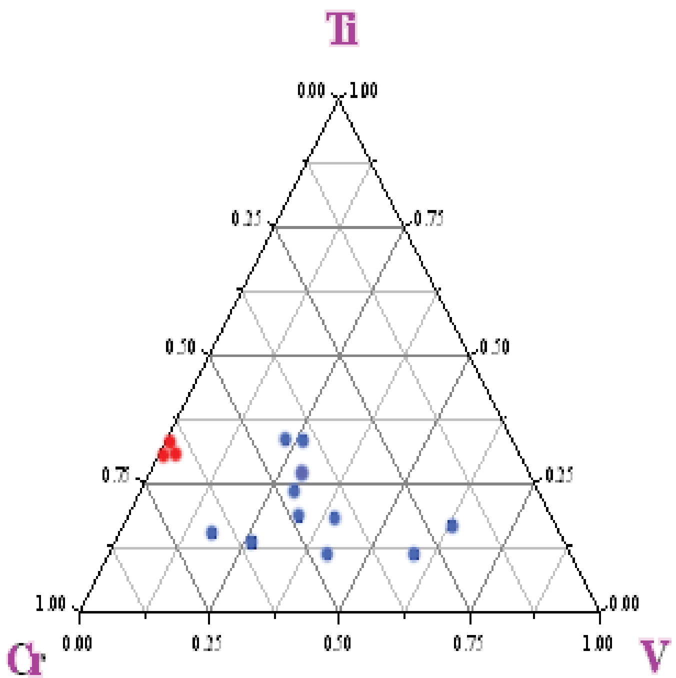

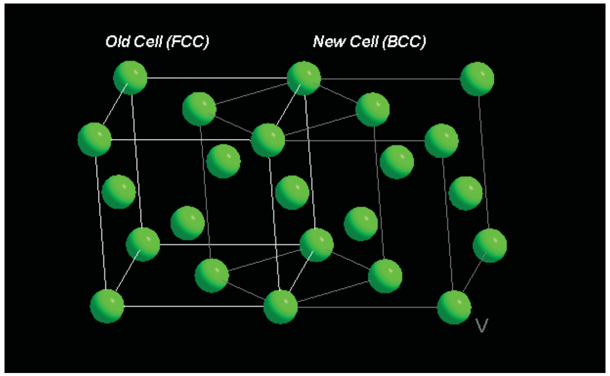

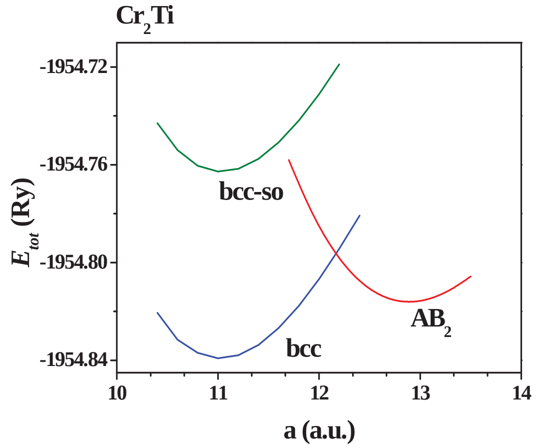

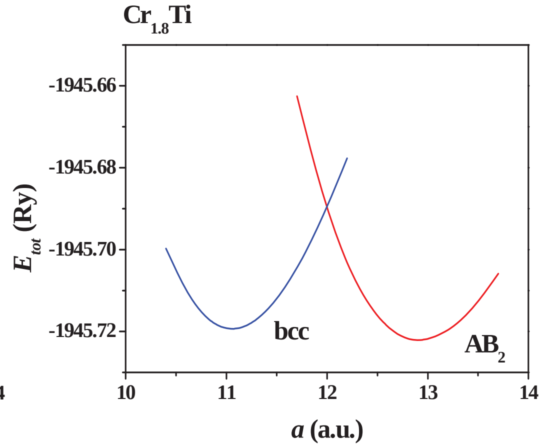

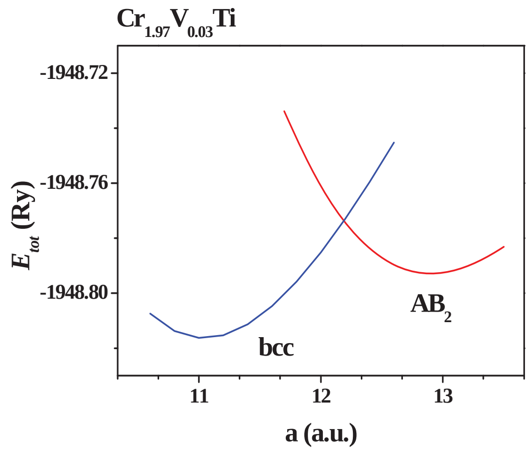

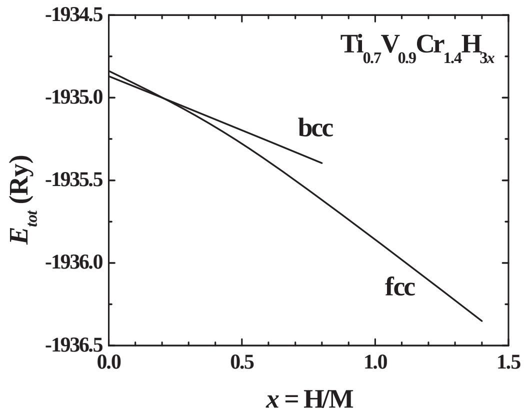

BCC type alloys (composite)

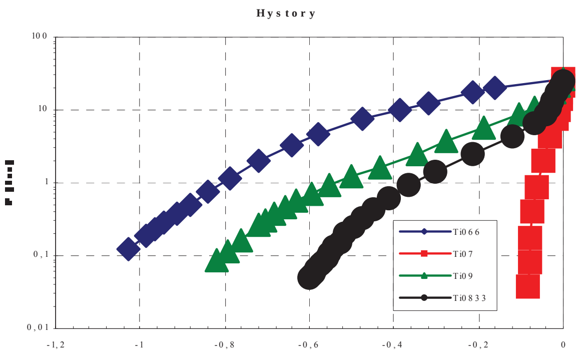

$TiV_{0.8}Cr_{1.2}$ x_{max} ~ 3.1w%.... up to…

$Ti_{0.5}V_{1.9}Cr_{0.6}$ x_{max} ~ 3.6w%

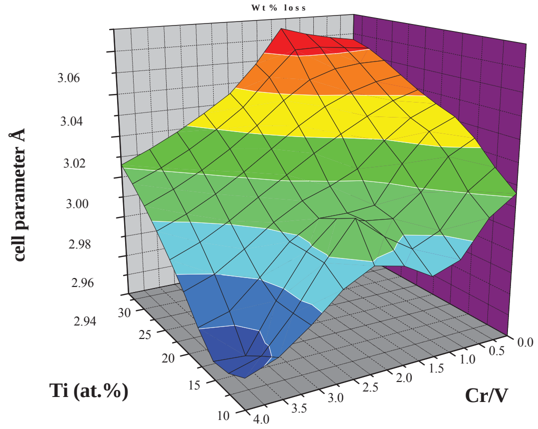

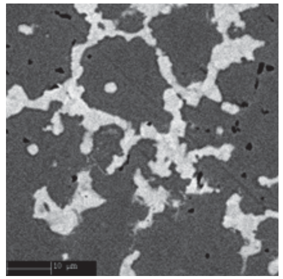

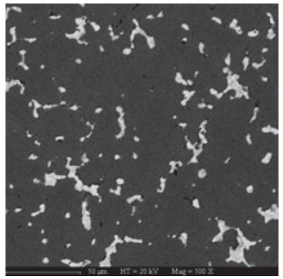

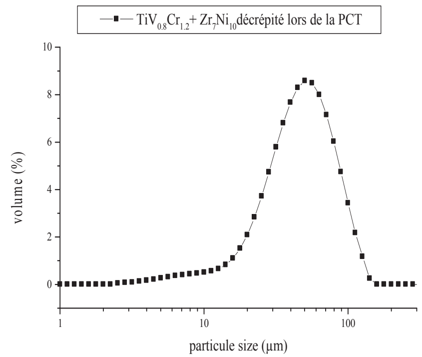

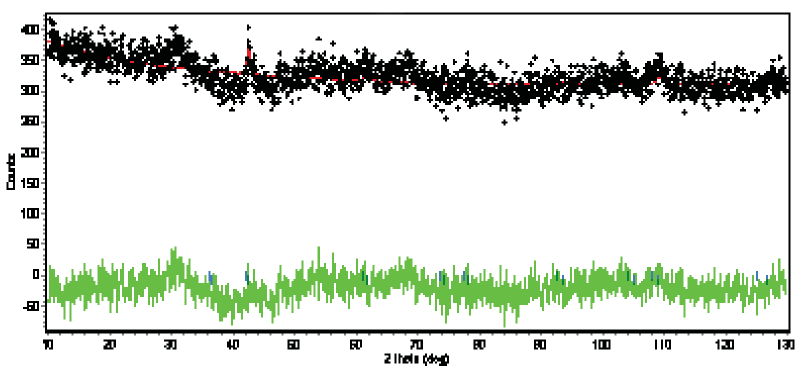

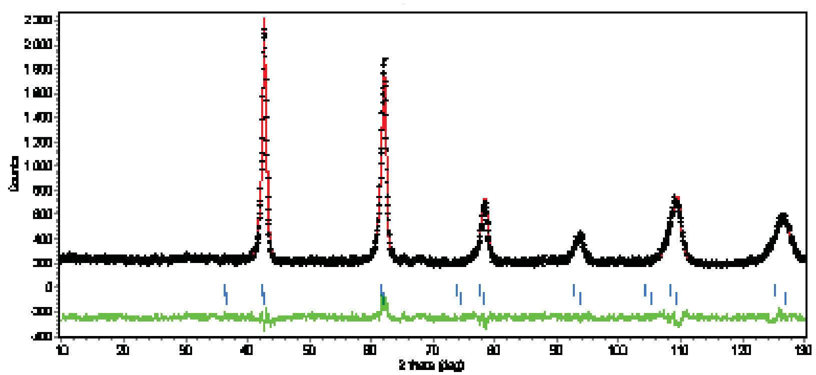

Mechanical and micro-structure modifications

Decrepitation:

In principle no change of formula, no transport of elements **(HD)**

Intergranular decrepitation

Intragranular decrepitation

Disproportionation:

Hydrogen Disproportionation Dehydrogenation Recombination **(HDDR)**

(magnet materials, hydrogen electrode materials)

Amorphisation:

Hydrogen Induced Amorphisation **(HIA)**

(shape memory materials, soft nanocrystallized materials)

Magnetic properties: intrinsic/extrinsic fundamentals

Atomic scale — Valence & conduction bands… involved in M-H

Spin (self rotation of electron) S_i

Orbit (orbital rotation of electron) L_i $J_i = L_i \pm S_i$

Magnetocrystalline anisotropy (Electric Field Gradient : EFG)

~ charge density of neighbour atoms coupling with the hyperfine field

Exchange force $E \sim J_{exch}$ $T_C \sim S_i \cdot J_{exch} \cdot S_j.$

nm to µm scale

Dipolar field

demagnetizing field / domain walls — Pinning by interstitials

Superparamagnetic / domain walls — Pinning by interstitials

Transition metal magnetism (alloys)

weak to strong ferromagnetic character

the first one type being more particularly volume (d-d distance) sensitive

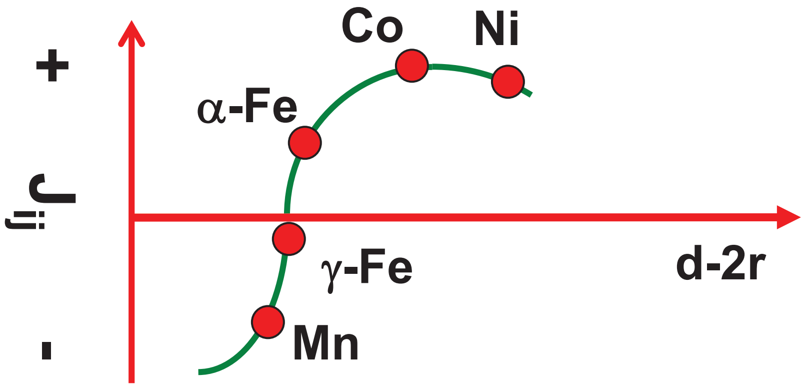

$T_C \sim J_{ij}\, S_i \cdot S_j$

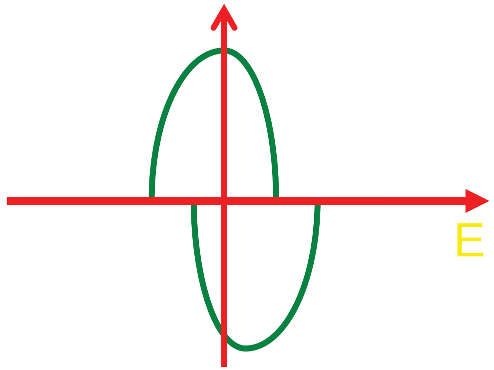

weak ferromagnet

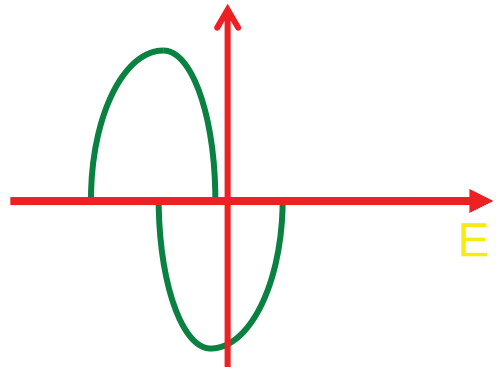

strong ferromagnet

Rare earth metal magnetism

Localized magnetism : discrete levels, not bands

$J = L \pm S$ spin and orbit components

exchange interaction via conduction electron density (s,d): metal-insulator trans.

RKKY mechanism : $E_{exch} \sim M_i \,.\, J_{RKKY} \,.\, M_j$

rather to very low T_C, very complex magnetic structures
very sensitive to M-H(s) bonds

otherwise magnetic to non magnetic transitions
or metal to insulator transitions
are induced at hydride formation

External pressure vs negative pressure effects

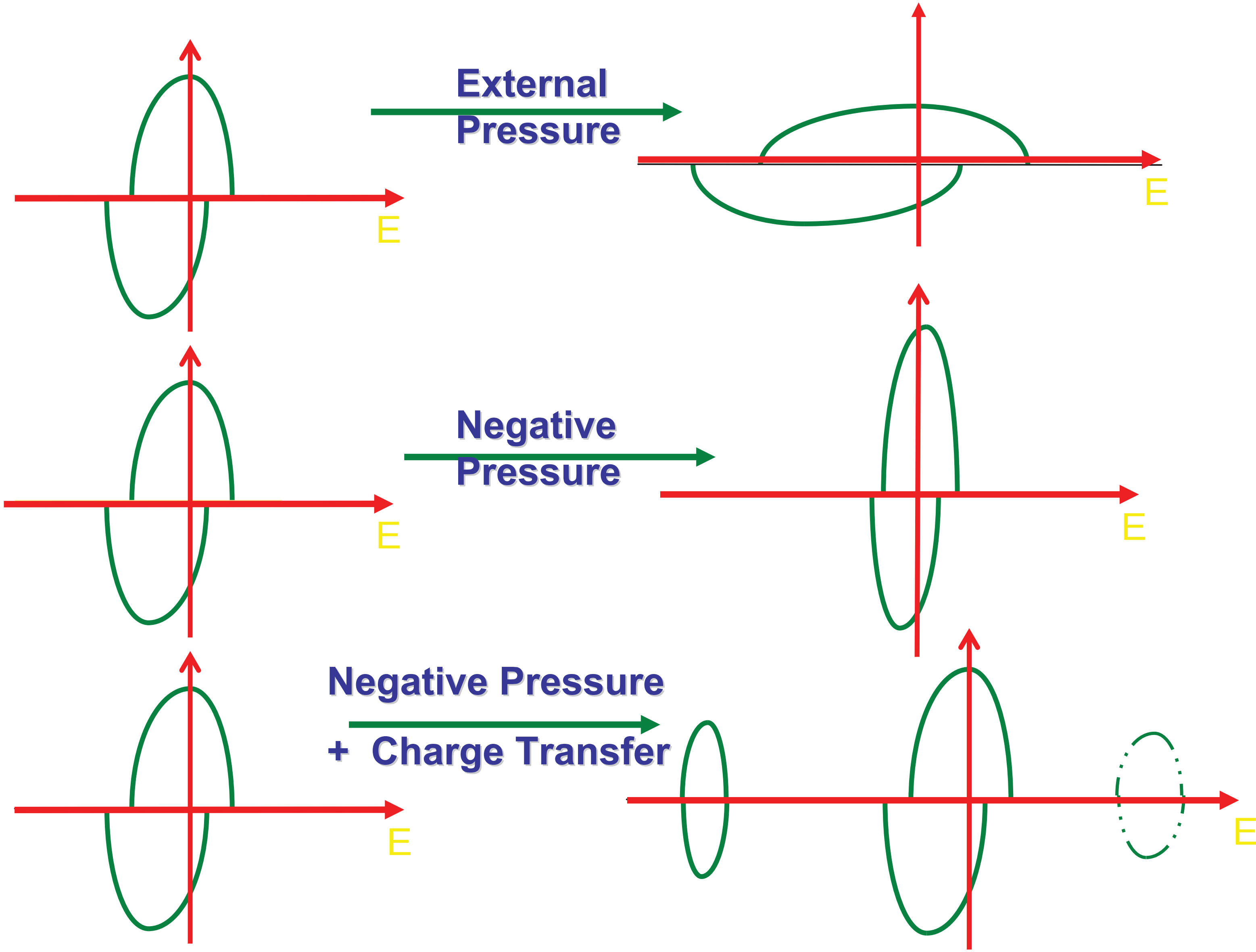

High pressure machines

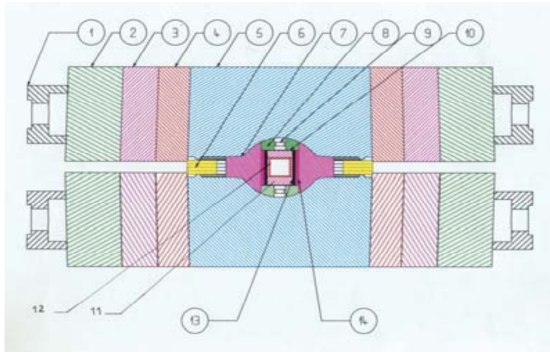

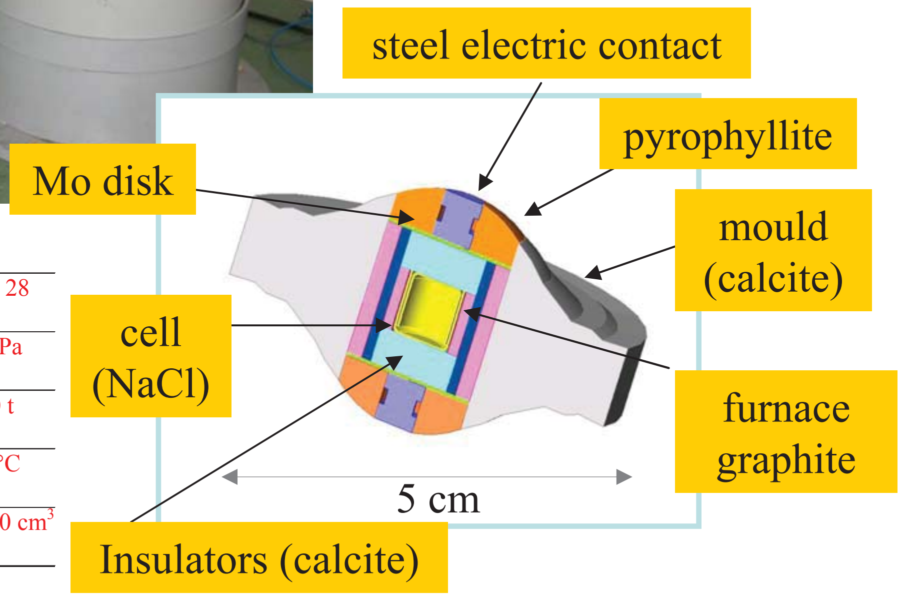

	Belt 12 mm	Belt 17 mm	Conac 40	Conac 28
	8 GPa	4 GPa	6 GPa	7.5 GPa
	180 t	230 t	1500 t	1000 t
	1500°C	1500°C	1500°C	1500°C
	0.04 cm^3	0.17 cm^3	0.80 - 1 cm^3	0.17- 0.40 cm^3

Superabundant vacancies (SAV) in Pd, Ni, Mn…
a new metal state…?

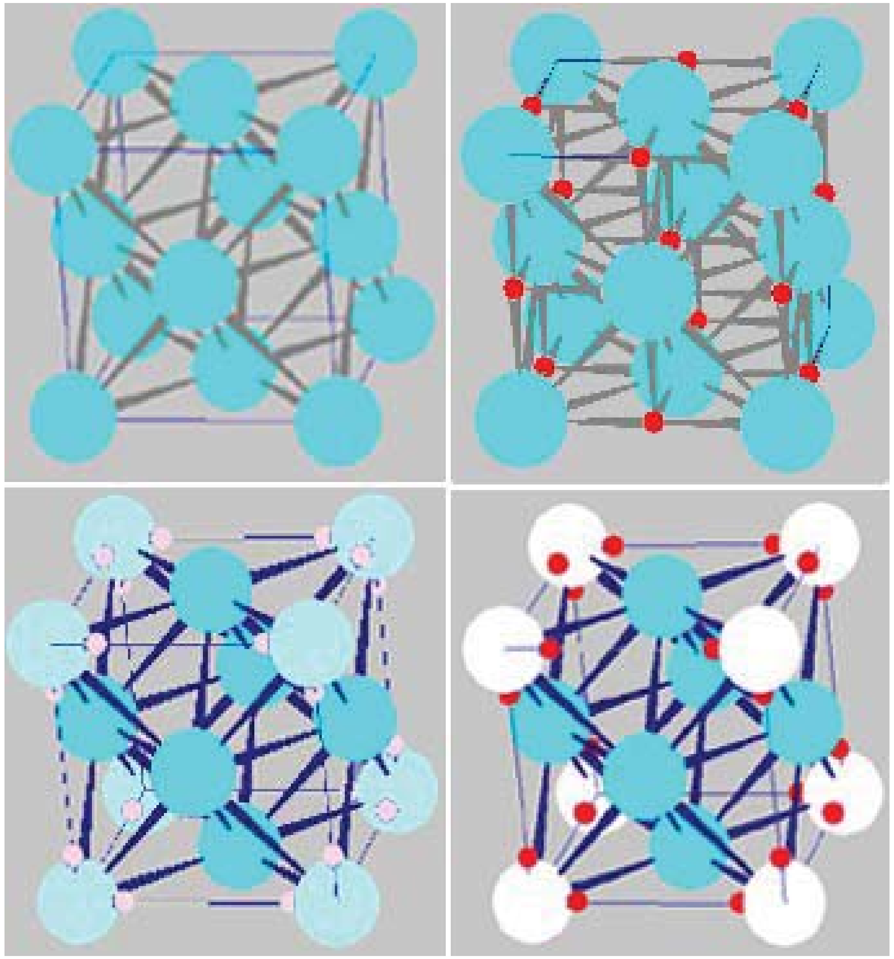

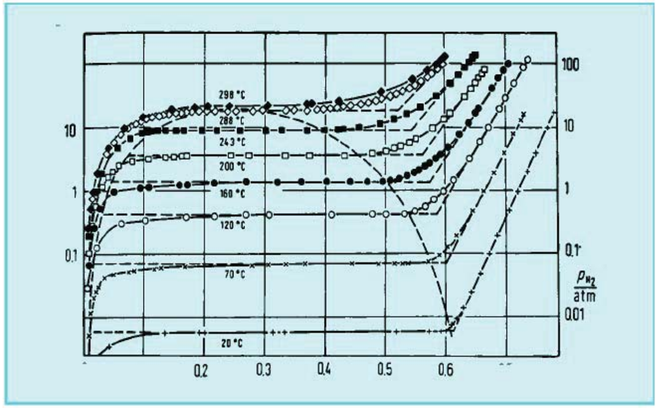

Diagramme d'état Composition-Pression à différentes températures du système palladium-hydrogène. La courbe de décomposition spinodale est clairement préfigurée par l'ensemble des isothermes.

DIMENSIONS :

H : 7 mm;   ϕ : 7 mm
épaisseur des parois de NaCl : 1 mm
épaisseur disque de métal : 0.1-0.2 mm
èpaisseur disque BN : 0.1 0.2 mm

Structure, properties and DOS calculations on SAV systems

Experiments at ESRF using the same set-up

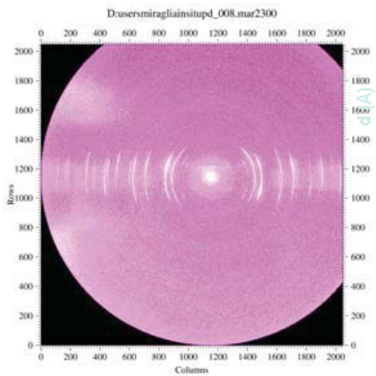

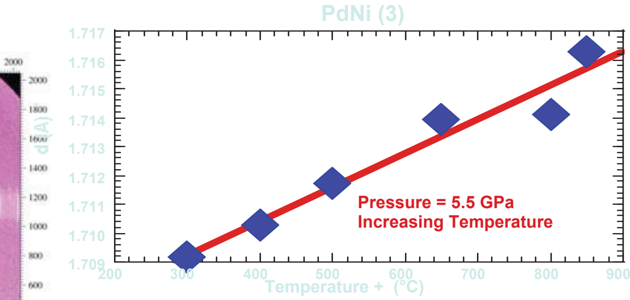

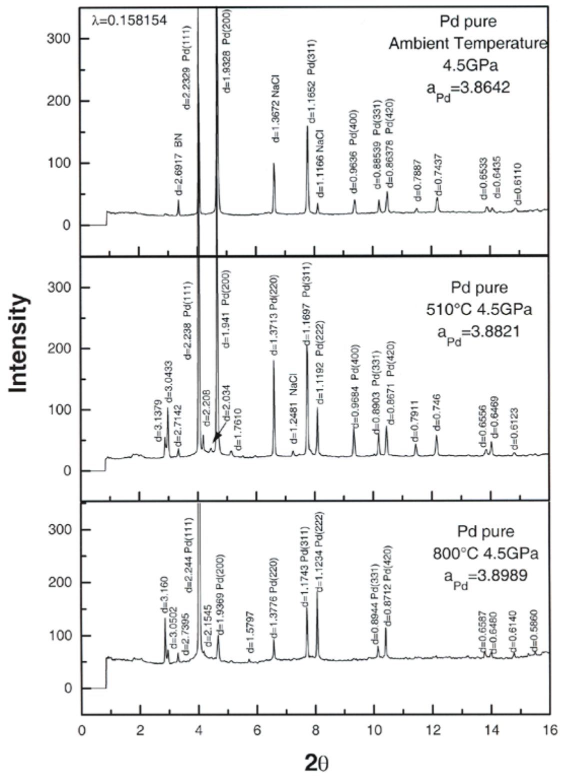

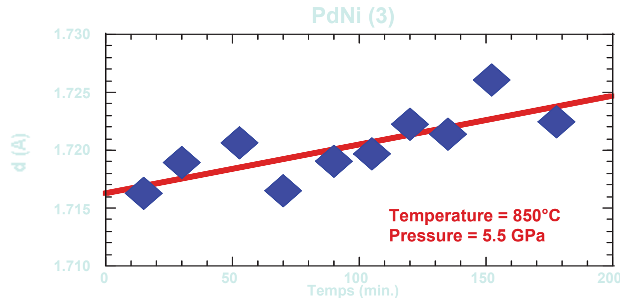

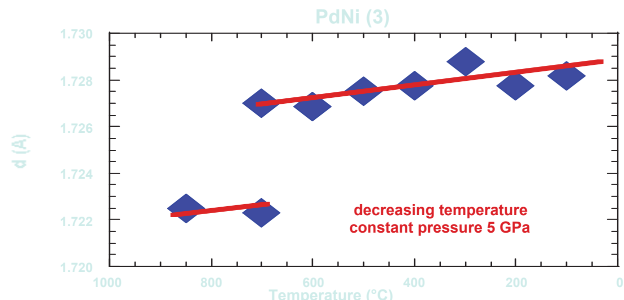

Structure, properties and DOS calculations on SAV systems

Pd - nearly ferromagnet
$PdH_{0.8}$ – superconductor 11 K
$Pd(Vac)H_2$ – AF correlations

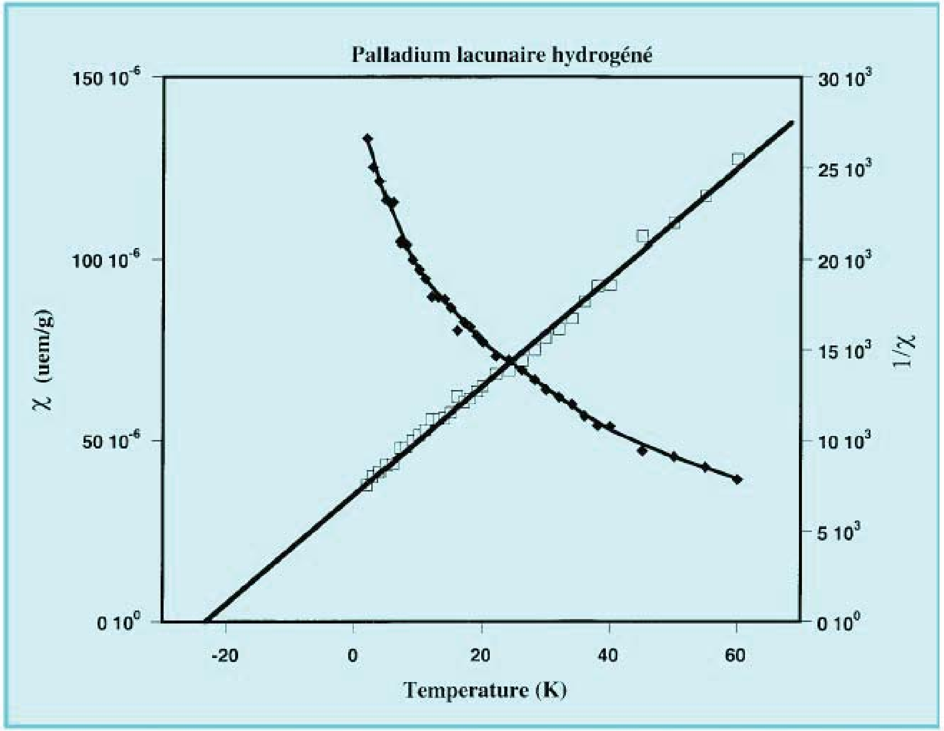

Susceptibilité magnétique et susceptibilité inverse du palladium lacunaire hydruré ($Pd_3(\square\text{-}H_x)$).

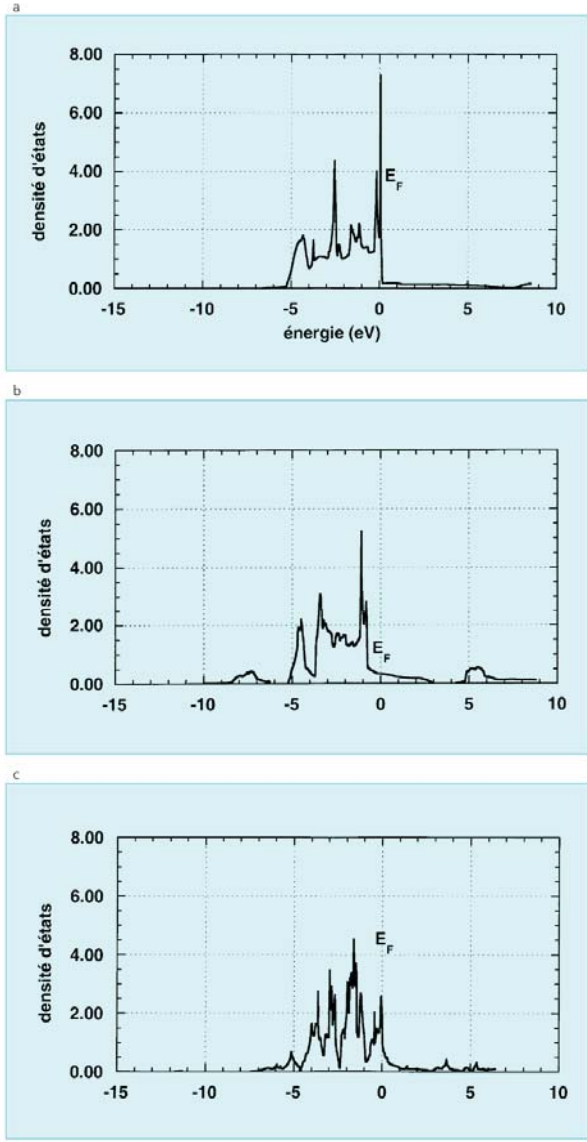

Densité d'états totale sur l'atome de palladium, calculée avec le code FLAPW.
a. pour le palladium métal (en bas),
b. le palladium hydruré « classique » $Pd_{H(x<1)}$, (au milieu),
c. le palladium lacunaire hydruré ($Pd_3(\square\text{-}H_x)$), (en haut).

Porous metal membranes - SAXS

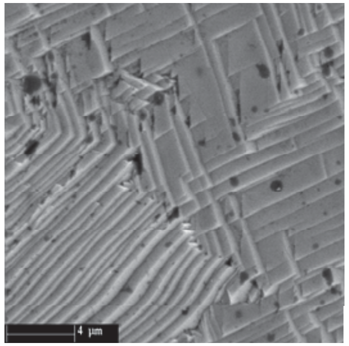

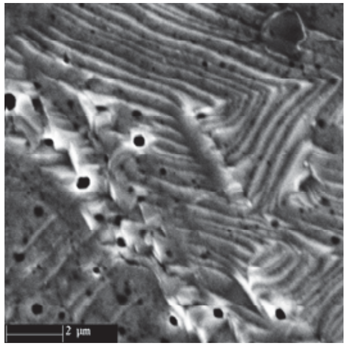

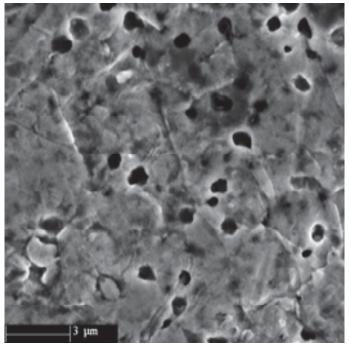

Vacancies coalesce along the defect pathes to forme pores
Behaviour of the pore size and distribution versus annealing temperature

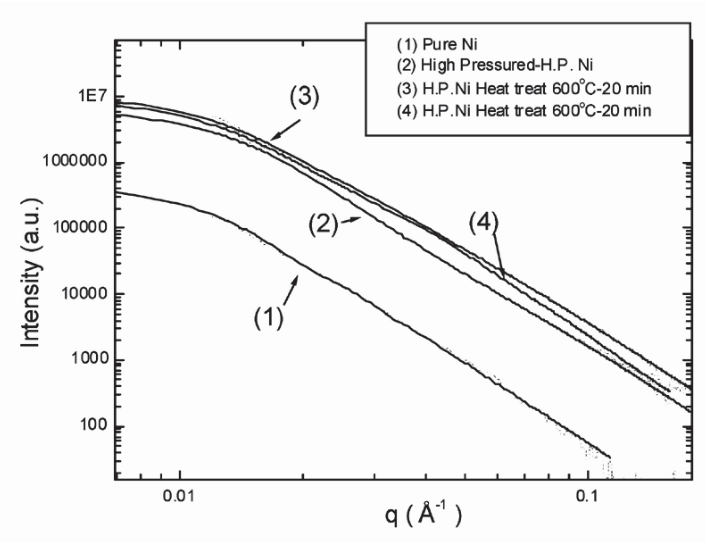

SAXS curves obtained for Ni submitted to a HHP of 3.5 GPa at 800 °C for 5 h, and subsequently heat treated at 600 °C for 20 and 40 min.

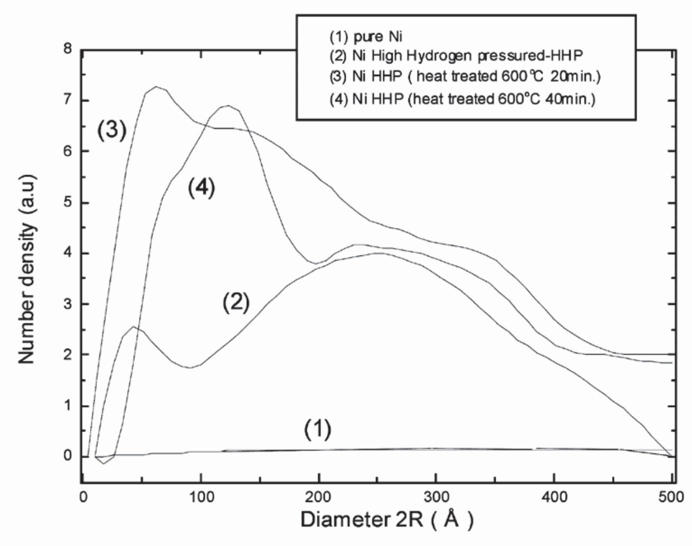

Size distribution of nanopores in Ni submitted to a HHP of 3.5 GPa at 800 °C for 5 h, and subsequently heat treated at 600 °C for 20 and 40 min.

Expitaxial interfaces of mixed catalysts from SAV assisted demixtion as seen by HREM & EXAFS

Very high H_2 pressure demixtion of alloys then controlled oxidization:
$(Pd_{0.8}Rh_{0.2})_{0.97}Ce_{0.03}$, $Pd_{0.97}Al_{0.03}$ and $(Pd_{0.9}Pt_{0.1})_{0.97}Al_{0.03}$)

Development of oxides nano-crystals in a platinoid matrix (both catalysts)

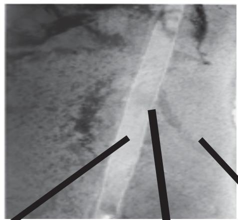

CeO_{2-x} épitaxed on Pd

Pd matrix

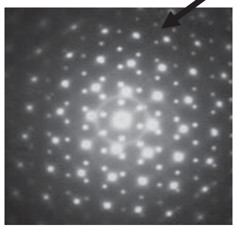

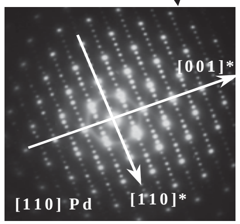

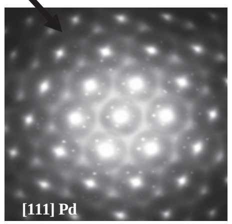

Antiphase structure Ce-O & PdO

Diluted cluster Ce (2%)

EXAFS

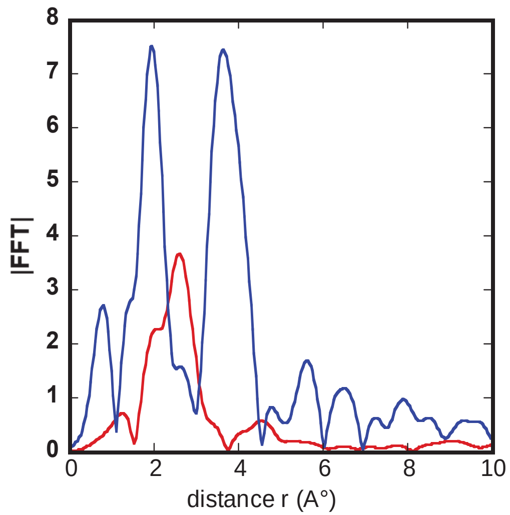

Before oxidization : S. Sol.
After oxidization : CeO_{2-x}

Ageing functional steels

Special steels for very deep off-shore oil diging

C : 0,41 - Cr : 25,5 - Ni : 34,9 - Mn : 1,03
Si : 1,91 - Nb : 0,78 - Ti : 0,04 - Fe : balance

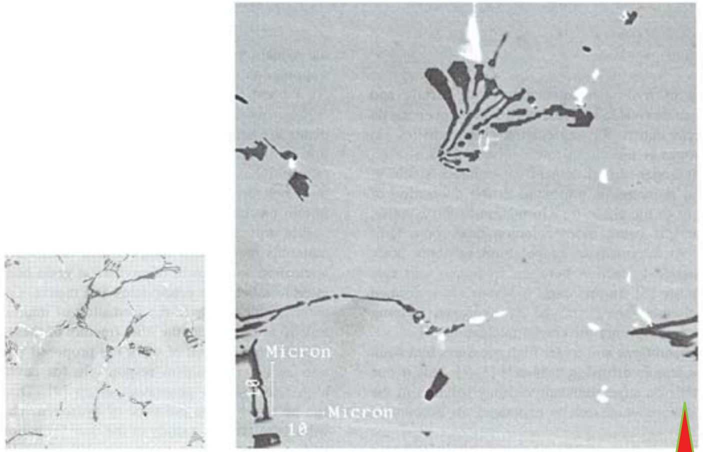

Typical micrograph of the HP 45 stainless steel with Nb and Ti additions in the as-cast condition.

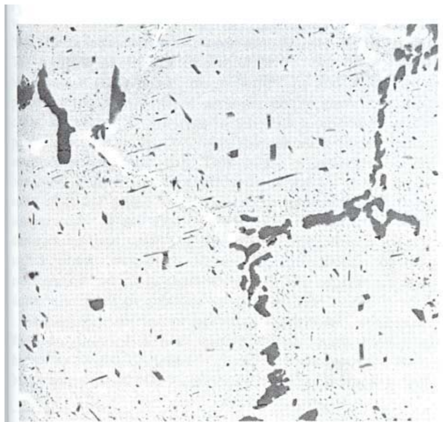

Microstructure of the HP 45 stainless steel after treatment with a low hydrogen pressure of 0.1 Pa for 100 h at 1200 K.

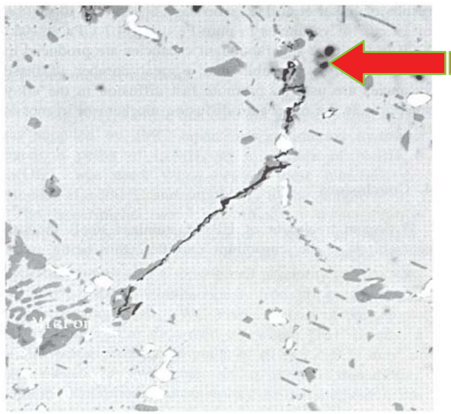

Microstructure of the HP 45 stainless steel after treatment with a high-hydrogen pressure of 5 GPa for 1 h at 873 K.

100 to 1000 hours treatment at ~ 1200 K under 0,1 Pa H_2 to simulate 2 years of steel ageing. Grain boundaries precipitates of the same ageed fragile phase were prompted within 1 h under 5 GPa H_2 at T < 900 K

Microwave assisted plasma deposits and implants

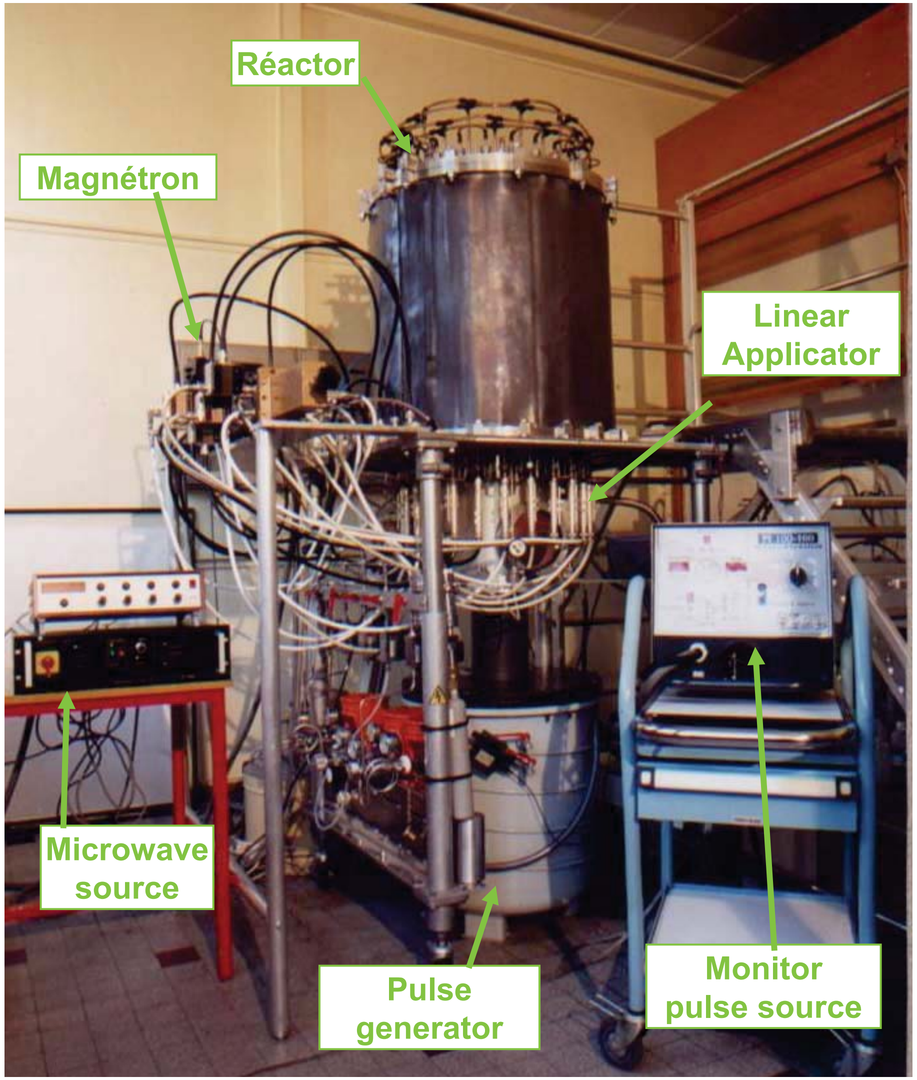

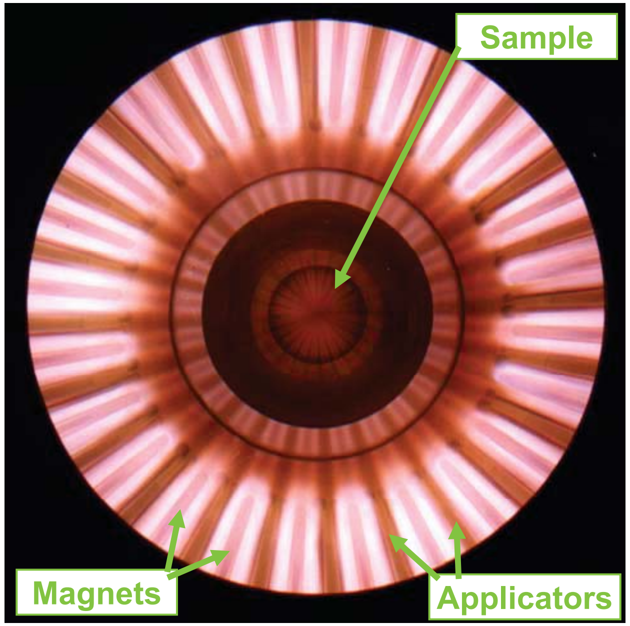

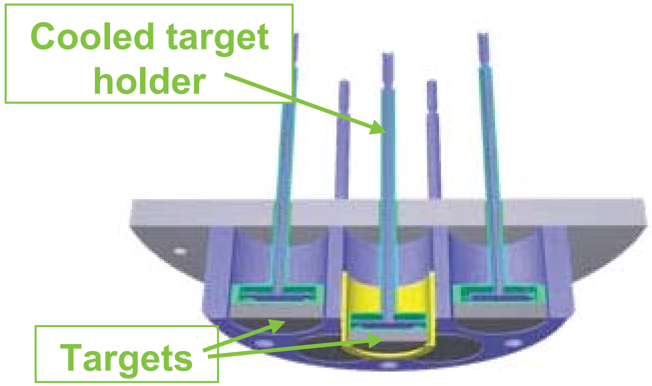

Porous foil e.g. Ni

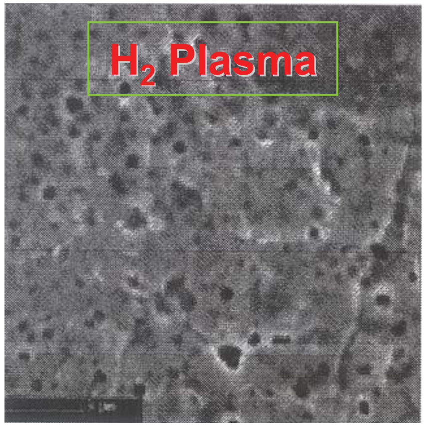

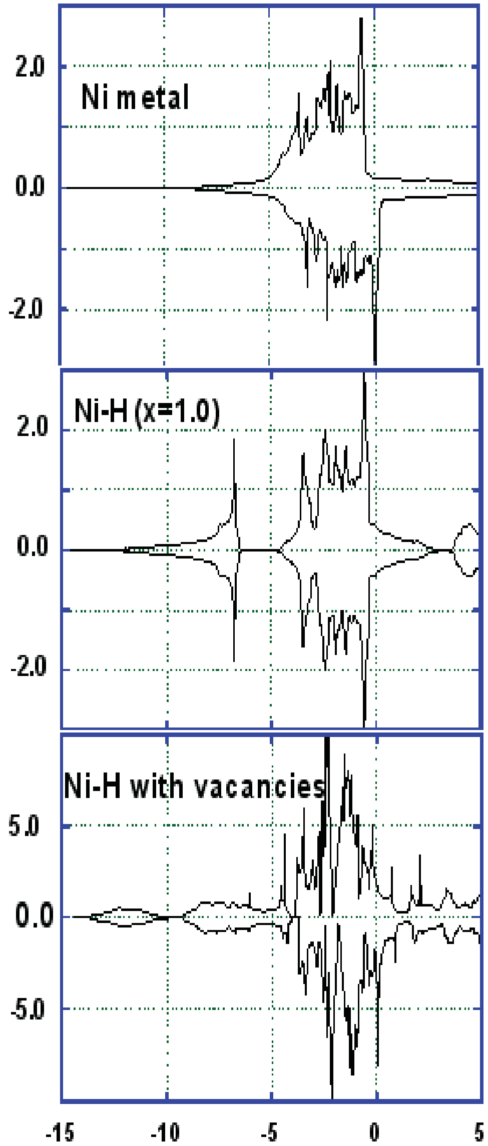

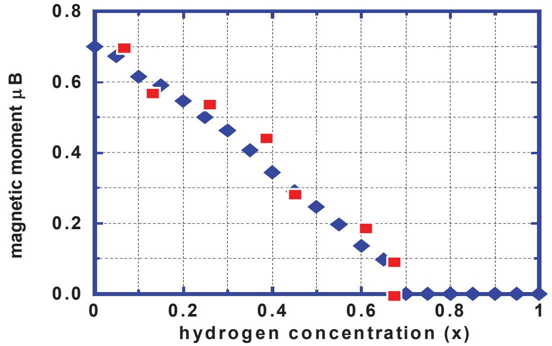

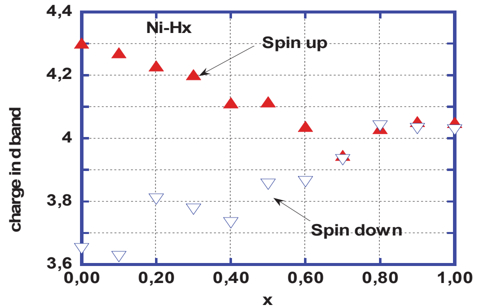

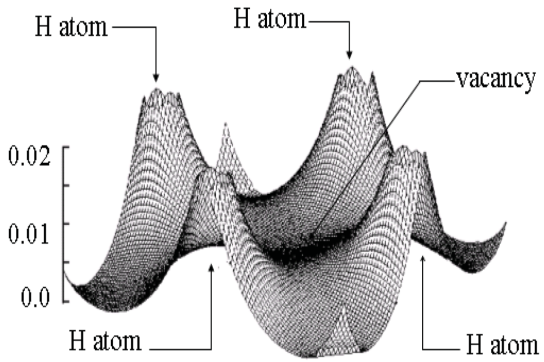

Switchable mirrors

Laser ablation

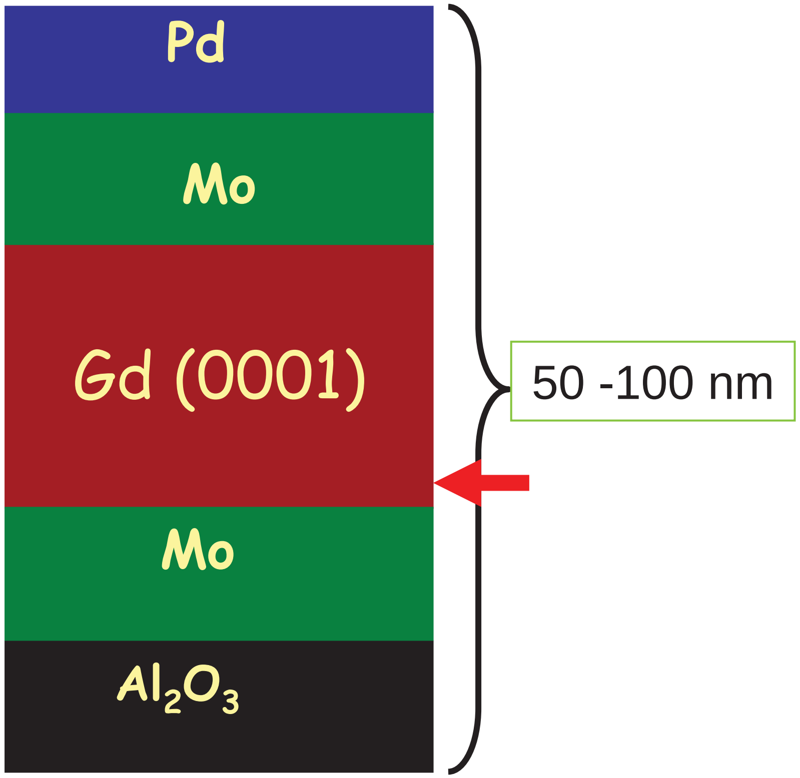

Switchable mirrors

GdH_3 as a quasi-semi conductor

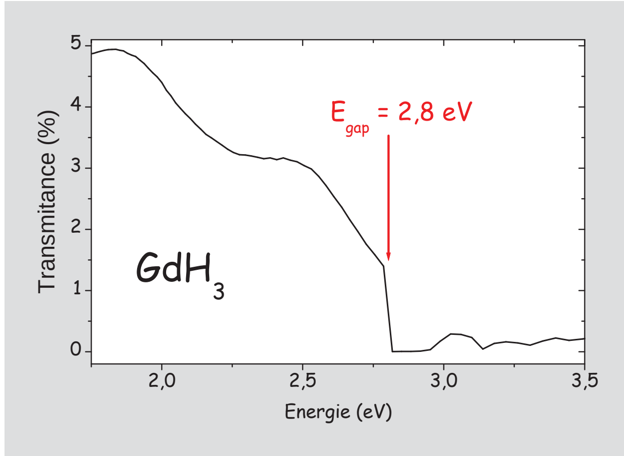

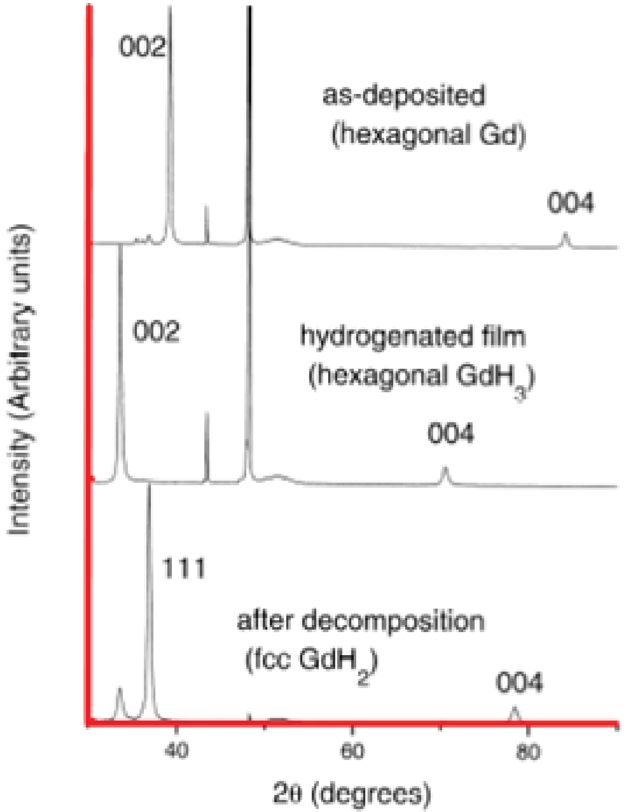

X-ray diffraction patterns of an as-deposited film (top), a hydrogenated film (center) and a film after decomposition (bottom).

Grazing XRD of HCP-Gd, FCC-GdH_2 and HCP GdH_3

Magnetization of Gd and $GdH_{\sim 3}$

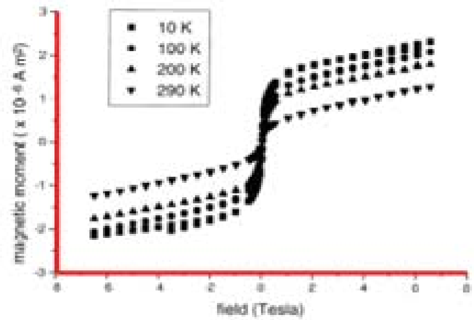

Magnetization curves for an as-deposited film.

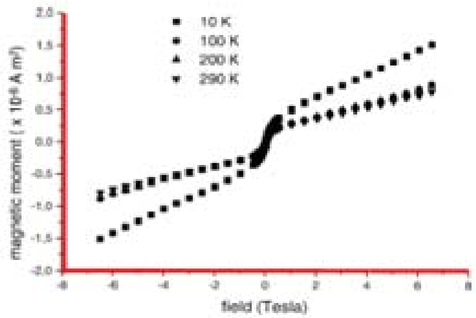

Magnetization curves for a hydrogenated film.


Neutron & synchrotron scattering facilities
NEUTRONS
FOR SCIENCE
ESRF (Synchrotron)
Thank you very much
for your kind attention
NÉEL
institut
Grenoble, France